P-even, *CP*-violating signals in scalar-mediated processes

Howard E. Haber,[1,*] Venus Keus,[2,†] and Rui Santos[3,4,‡]

[1]*Santa Cruz Institute for Particle Physics, University of California, Santa Cruz, California 95064, USA*
[2]*Dublin Institute for Advanced Studies, School of Theoretical Physics, 10 Burlington road, Dublin D04 C932, Ireland*
[3]*Centro de Física Teórica e Computacional, Faculdade de Ciências Universidade de Lisboa, Campo Grande, Edifício C8, 1749-016 Lisboa, Portugal*
[4]*ISEL—Instituto Superior de Engenharia de Lisboa Instituto Politécnico de Lisboa, 1959-007 Lisboa, Portugal*

(Received 29 June 2022; accepted 12 October 2022; published 30 November 2022)

Most studies of Higgs sector *CP* violation focus on the detection of *CP*-violating neutral Higgs-fermion Yukawa couplings, which yield *P*-odd, *CP*-violating phenomena. There is some literature on purely bosonic signatures of Higgs sector *CP* violation, where the simultaneous observation of three processes (suitably chosen) constitutes a signal of *P*-even *CP* violation. However, in the examples previously analyzed, some of the processes are strongly suppressed in the approximate Higgs alignment limit (corresponding to the existence of a Standard Model-like Higgs boson as suggested by LHC data), in which case the proposed *CP*-violating signals are difficult to observe in practice. In this paper, we extend the existing literature by examining processes that do not vanish in the Higgs alignment limit and whose simultaneous observation would provide unambiguous evidence for scalar-mediated *P*-even *CP* violation. We assess the discovery potential of such signals at various future multi-TeV lepton (and $\gamma\gamma$) colliders. The potential for detecting loop-induced *P*-even, *CP*-violating phenomena is also considered.

DOI: 10.1103/PhysRevD.106.095038

I. INTRODUCTION

The Higgs boson of the Standard Model (SM) is a *CP*-even scalar. Strictly speaking, this statement is only approximately true, since the SM Lagrangian is not *CP* conserving due to the presence of an unremovable complex phase in the Cabibbo-Kobayashi-Maskawa (CKM) matrix. This phase will generate *CP*-violating observables in processes involving the Higgs boson via radiative corrections. However, in practice, any such contributions are extremely tiny and can be neglected.

There have been a number of theoretical motivations advanced in the literature that suggest the existence of additional scalar degrees of freedom beyond the Higgs boson of the SM. However, even independently of such motivations, it is striking to observe that the fermion and gauge sectors of the SM are nonminimal. Thus, if the scalar sector of the SM follows a similar pattern, then one should expect the existence of additional Higgs scalars in nature. Perhaps some of these scalars will possess masses that are not significantly larger than the observed Higgs boson, in which case they may be discoverable at the LHC or at future hadron and/or lepton colliders now under consideration.

Current LHC data already place nontrivial restrictions on the structure of an extended Higgs sector. First, the observation that the electroweak ρ parameter is very close to 1 suggests that any extended Higgs sector is most likely composed of hypercharge $Y = \pm 1$ doublet fields (and perhaps singlet fields) with respect to the electroweak gauge group.[1] Second, the LHC Higgs data have already achieved a precision that implies that the properties of the observed Higgs boson closely approximate those of the SM Higgs boson to within an accuracy that is typically in the range of 10%–20% depending on the observable [2,3].

*haber@scipp.ucsc.edu
†venus@stp.dias.ie
‡rasantos@fc.ul.pt

Published by the American Physical Society under the terms of the Creative Commons Attribution 4.0 International license. Further distribution of this work must maintain attribution to the author(s) and the published article's title, journal citation, and DOI. Funded by SCOAP[3].

[1]We have chosen a convention, such that $Q = T_3 + \frac{1}{2}Y$, where Q is the electric charge, T_3 is the third component of the weak isospin, and Y is the hypercharge. Note that if other scalar multiplets are included, then (in most cases) the Higgs sector parameters must be fine tuned to achieve $\rho \simeq 1$, in contrast to extended Higgs sectors consisting of $Y = 0$ singlet and $Y = \pm 1$ doublet scalar fields where the tree-level value of the ρ-parameter is automatically equal to 1. For further details and references to the original literature, see Ref. [1].

The existence of a SM-like Higgs boson in the scalar spectrum implies that the Higgs sector is close to the so-called Higgs alignment limit [4–9].

Consider an extended Higgs sector with n hypercharge-1 SU(2) doublet scalar fields Φ_i and m additional hypercharge-0 singlet scalar fields ϕ_i. After minimizing the scalar potential, we assume that only the neutral scalar fields acquire nonzero vacuum expectation values (vevs), thereby preserving $\mathrm{U}(1)_{\mathrm{EM}}$, with $\langle\Phi_i^0\rangle = v_i/\sqrt{2}$ and $\langle\phi_j^0\rangle = x_j$, where $v^2 \equiv \sum_i |v_i|^2 = (\sqrt{2}G_F)^{-1} \simeq (246\ \mathrm{GeV})^2$ and G_F is the Fermi constant of weak interactions. One can then introduce new linear combinations, H_i, which define the so-called *Higgs basis* [10–15]. In particular,

$$H_1 = \begin{pmatrix} H_1^+ \\ H_1^0 \end{pmatrix} = \frac{1}{v}\sum_i v_i^* \Phi_i, \qquad \langle H_1^0\rangle = v/\sqrt{2}, \quad (1)$$

and $H_2, H_3, \ldots, H_n$ are the other mutually orthogonal linear combinations of doublet scalar fields such that $\langle H_i^0\rangle = 0$ (for $i \neq 1$). That is, H_1^0 is *aligned* in field space with the direction of the scalar field vev. In the exact Higgs alignment limit,

$$\varphi \equiv \sqrt{2}\mathrm{Re}H_1^0 - v \quad (2)$$

is a scalar mass eigenstate such that the tree-level couplings of φ to itself, to gauge bosons, and to fermions coincide with those of the SM Higgs boson. However, generically φ is *not* a scalar mass eigenstate due to its mixing with other neutral scalars. An approximate Higgs alignment limit, in which the Higgs sector contains a SM-like neutral Higgs scalar, is achieved if at least one of the following two conditions are satisfied: (i) the diagonal squared masses of $H_2, H_3, \ldots, H_n$ are all large compared to the squared mass of the observed Higgs boson (corresponding to the *decoupling limit* [5,16]), and/or (ii) the elements of the neutral scalar squared mass matrix that govern the mixing of φ with the other neutral scalar fields are suppressed.

The Higgs alignment limit is most naturally achieved in the decoupling regime, where the observed Higgs boson [whose mass is of $\mathcal{O}(v)$] is significantly lighter than all additional scalars of the Higgs sector. That is, a new mass parameter, $M \gg v$, exists that characterizes the mass scale of the additional scalars. After integrating out all the heavy degrees of freedom at the mass scale M, one is left with a low-energy effective theory that consists of the SM particles, including a single neutral scalar boson, which is identified with the SM Higgs boson. Alternatively, one can achieve approximate Higgs alignment if the mixing of φ with the other neutral scalars of the extended Higgs sector is suppressed. In this case, it is possible that additional scalar states with masses of $\mathcal{O}(v)$ are present in the scalar spectrum beyond the scalar state currently identified as the SM-like Higgs boson. This is the case of Higgs alignment without decoupling. It is typically achieved by fine tuning the parameters of the extended Higgs sector. However, in some special cases, exact Higgs alignment without decoupling can be implemented due to the presence of a symmetry [17–24]. For example, certain exact discrete symmetries can be imposed such that the mixing of the SM Higgs doublet with additional (so-called inert) scalar doublets is forbidden [25–34]. In such models, the tree-level properties of the 125 GeV Higgs boson coincide with those of the SM Higgs boson, corresponding to the exact Higgs alignment limit.

At present, no additional Higgs-like scalar states beyond the SM-like Higgs boson have been found at the LHC. Furthermore, the properties of the observed Higgs boson approximate those of the SM Higgs boson as noted above. Consequently, if additional Higgs bosons exist, then the Higgs alignment limit of the extended Higgs sector must be approximately realized. In this scenario, the detection of new neutral scalars[2] via couplings to gauge bosons is difficult due to the sum rule [35],

$$\sum_i \lambda^2_{VVh_i} = \lambda^2_{VVh_{\mathrm{SM}}}, \quad \text{for } VV = W^+W^- \quad \text{or} \quad ZZ, \quad (3)$$

that is satisfied in any extended Higgs sector with $\rho = 1$ and no $ZW^\pm H_i^\mp$ couplings at tree level.[3] In particular, Eq. (3) forces the couplings of h_i (for $i > 1$) to gauge bosons to be very small when $h_1 \simeq h_{\mathrm{SM}}$ is SM-like.

In models with extended Higgs sectors, there is a potential for new sources of CP violation arising in the scalar sector. Thus, if new scalar states are discovered at the LHC, it will be important to search for new signals of scalar-mediated CP-violating phenomena. In the approximate Higgs alignment limit, the observed Higgs boson will continue to behave as an approximate CP-even scalar. However, possible CP-violating phenomena associated with the additional scalar states of the Higgs sector can be present and may be observable. In this paper, we shall discuss various possible CP-violating observables associated with the extended Higgs sector.

Here, we provide two examples of CP-violating observables associated with the scalar sector. Consider the process $\gamma\gamma \to H$ mediated by a fermion loop. If the scalar state H is not an eigenstate of CP, then the $Hf\bar{f}$ vertex will be of the form

$$H\bar{f}(a + ib\gamma_5)f, \quad (4)$$

[2]In our notation, $h_1 \equiv h_1(125)$ is the observed Higgs boson of mass 125 GeV, and the h_i for $i \neq 1$ correspond to new neutral scalars of the extended Higgs sector.

[3]These conditions are automatically realized in extended Higgs sectors made up exclusively of $Y = 0$ singlet and $Y = \pm 1$ doublet scalars.

where a and b are real (as a consequence of Hermiticity of the effective interaction). The one-loop diagram for $H\gamma\gamma$ then yields an effective interaction

$$\mathcal{L}_{\rm int} = H(a'FF + b'F\tilde{F}), \tag{5}$$

where a' and b' are real, F is the photon field strength tensor, and $\tilde{F}$ is the dual field strength tensor. In particular, if $ab \neq 0$, then $a'b' \neq 0$, in which case the $H\gamma\gamma$ interaction is CP-violating and H is a scalar of indefinite CP quantum number. In this case, CP violation can be experimentally detected if the initial photon polarizations can be specified. For example, polarization asymmetries are defined in Ref. [36] that would provide an unambiguous signal of CP violation in the production of H. Such a process could be studied in a $\gamma\gamma$ collider mode of a future e^+e^- linear collider (using Compton backscattered laser beams). The initial photon polarizations are determined by the polarization of the initial electron and positron beams.

A second example makes direct use of the Higgs-fermion coupling given in eq. (4). For example, the energy distribution of the τ decay products in $H \to \tau^+\tau^-$ are correlated with the τ polarization. The end result is a nontrivial azimuthal angle correlation of the final state decay products that provides the CP-violating signal [37–41]. Finally, CP violation can also be probed in $\bar{t}tH$ production. Although the scalar and pseudoscalar amplitudes do not interfere, the cross section can be written as a function of $a^2 + b^2$ and $a^2 - b^2$, the latter being proportional to the top quark mass. In order to optimize the extraction of the $(a^2 - b^2)$ term, many variables have been proposed over the years; see e.g. Refs. [42–46].

The ATLAS and CMS collaborations have performed various studies to probe the CP nature of the 125 GeV Higgs boson in its couplings to top quarks and to τ leptons. Both experimental collaborations [47,48] employ the two photons decay channel $H \to \gamma\gamma$ in the production process $pp \to t\bar{t}H$ and attempt to measure a CP-violating mixing angle defined as $\theta \equiv \arctan(b/a)$, where a and b are given in eq. (4). The purely CP-odd hypothesis is excluded at the level of 3.9 standard deviations, and an observed (expected) exclusion upper limit at 95% C.L. was obtained for the mixing angle of $\theta = 43°$ (63°). Using data collected at $\sqrt{s} = 13$ TeV (with an integrated luminosity of 137 fb^{-1}), the CMS Collaboration [49] has recently measured the CP mixing angle of the tau lepton, $\theta = 4° \pm 17°$, while setting an observed (expected) exclusion upper limit of 36° (55°).

In both of the examples cited above, the actual experimental observable violates P and CP while preserving C. That is, in the case of eq. (4), $\bar{f}f$ and $i\bar{f}\gamma_5 f$ are C-even bilinear covariants. Hence, if one identifies H as a C-even state, then the $H\bar{f}f$ vertex is C conserving. Likewise, the photon is a C-odd state so that both FF and $F\tilde{F}$ are C-even operators, which implies that the effective interaction given by eq. (5) is C even. Of course, C is not a good quantum number of the SM; it is violated by W and Z mediated interactions. However, in the context of the examples presented above, the effects of the C-violating W and Z mediated interactions only appear via radiative corrections. Thus, in first approximation, we may treat eq. (5) as a C-conserving interaction.

The examples above, where the CP-violating interactions of the scalars are attributed to approximately C-conserving, P-violating interactions, originate from the structure of the Higgs-fermion couplings. However, there is an alternative possibility in which the CP-violating interactions of the scalars are attributed to approximately C-violating, P-conserving interactions that originate from the structure of the bosonic couplings of the Higgs bosons (these include the Higgs couplings to vector bosons and the Higgs boson self-couplings).

In this paper, we shall focus on this second class of CP-violating signals in the scalar sector that arise from P-even, CP-violating interactions. One example of this phenomenon, which is well studied in the literature [50–54], involves the coupling of the Z boson to a pair of neutral scalars h_i via the Zh_ih_j vertex ($i < j$). Since the pair of scalars that couples to a spin-1 boson has relative orbital angular momentum equal to 1, it follows that h_ih_j must be a CP-odd state. In the two Higgs doublet model (2HDM) where $i = 1, 2, 3$, if all three possible combinations of Zh_ih_j for $i < j$ are observed, then CP must necessarily be violated. Experimentally, these couplings can be probed by either observing the three decays $h_3 \to h_2Z$, $h_3 \to h_1Z$, and $h_2 \to h_1Z$ or the production processes $Z^* \to h_3h_2$, $Z^* \to h_3h_1$, and $Z^* \to h_2h_1$ via s-channel Z boson exchange. As shown in Refs. [52,54], the three scalar decays, if kinematically allowed, would be visible at future LHC runs in a significant portion of the parameter space. In contrast, the identification of the production of scalar pairs via s-channel Z exchange is significantly more difficult at a hadron collider because other production mechanisms, such as gluon initiated processes via top and bottom quark loops, tend to dominate [55].

Moreover, the viability of the P-even, CP-violating signal discussed above depends on appreciable Zh_ih_j couplings for all possible $i < j$. However, since h_1 is identified as the observed SM-like Higgs boson, the Zh_1h_j ($j \neq 1$) couplings all vanish in the exact Higgs alignment limit, and the CP-violating signal is completely lost. In the approximate Higgs alignment limit, the suppression of the corresponding Zh_1h_j ($j \neq 1$) couplings limits the usefulness of the P-even, CP-violating signal. Thus, one must either rely on a set of Zh_ih_j couplings where $i \neq 1$ and $j \neq 1$ (which would require an extended Higgs sector beyond two doublets) or else search for alternative CP-violating signals that are not suppressed in the Higgs alignment limit.

Any search for scalar-mediated P-even, CP-violating phenomena can be contaminated by fermionic P-violating

contributions in the production process. If no evidence is found for all three vertices Zh_ih_j $(i < j)$ by end of the high-luminosity stage of the LHC, then one may conclude that at least one (or more) of the following statements must hold: (i) there are no new scalars beyond the SM Higgs boson that are kinematically accessible at the LHC; (ii) some or all of the bosonic decays of h_2 and h_3 are not kinematically allowed; and/or (iii) the departure from the Higgs alignment limit deduced from the precision Higgs data is so severe that the suppression of the three vertices precludes their observation at the LHC.

For a robust interpretation of the signal for P-even CP violation, one should ensure that there is no contamination of the P-even, CP-violating signal due to effects from the neutral Higgs-fermion interactions, either via the production process or from competing contributions to the bosonic vertices. In this paper, we will eliminate possible contamination due to CP-violating neutral Higgs-fermion Yukawa couplings by focusing on the production of Higgs bosons at a high energy lepton collider, with a focus on the bosonic Higgs vertices that arise at tree level and are unsuppressed in the Higgs alignment limit.

The assertion above that the existence of three couplings of the form Zh_ih_j $(i < j)$ can be interpreted as a P-even, CP-violating observable requires some elucidation. In Sec. II, we demonstrate that in a CP-conserving gauge theory of scalars and gauge bosons where the fermions are excluded, C and P are separately conserved. In this case, we are free to set $P = +1$ for *all* scalars, in which case the presence or absence of the Zh_ih_j coupling is determined completely by the C properties of the Higgs bosons and gauge bosons. As an example, it is instructive to employ the 2HDM with the fermions omitted since CP-violating phenomena arising in this theory are associated with P-even, CP-odd observables.

In Sec. III, we examine a class of P-conserving, C-violating processes involving scalars of an extended Higgs sector that can be used to identify the presence of scalar-mediated CP violation. In this analysis, we initially focus on processes that are not suppressed in the Higgs alignment limit. We then identify both tree-level and loop-induced processes that can provide evidence for CP violation. In any realistic application, loop-induced processes may include "fermion pollution"—that is, contributions from fermion loops that can complicate the interpretation of the CP-violating signal. Thus, we focus primarily on tree-level purely bosonic P-odd, CP-violating phenomena, where the effects of the Yukawa interactions can only enter via small radiative corrections.

In Sec. IV, we study the discovery potential of our proposed observables at future lepton (both e^+e^- and $\mu^+\mu^-$) and photon colliders. We calculate the relevant cross sections and estimate the total number of signal events for each observable for a given set of Higgs sector parameters. Future lepton colliders with a center of mass energy of a few TeV are better suited for the s-channel processes, whereas two photon processes only become relevant at energies above 10 TeV.

An indirect way to detect the presence of P-even CP violation is to probe the loop contributions to the triple Z form factor [56]. CP-violating contributions to the triple gauge boson vertices ZZZ and ZW^+W^- vertices were first studied in Refs. [57–60]. The Lorentz structure of the general ZZZ and ZW^+W^- vertices contains seven independent form factors, one of which (denoted by f_4) measures the P-even, CP-violating contribution to the vertex. The possible contribution of the extended Higgs sector to f_4 is discussed in Sec. V. Loop processes are also relevant in Sec. VI, where we examine P-even, CP-violating observables with multiple photons and/or Z bosons in the final state (with some details relegated to Appendix B). Unfortunately, such signals will be very difficult to nearly impossible to detect in any future experimental program.

Although our examples are presented in the context of the Higgs alignment limit, in some cases, one can tolerate some suppression factors that arise if the Higgs alignment limit is only approximately realized. In Sec. VII, we classify additional signals of P-even, CP-odd observables that can be employed if deviations from the exact Higgs alignment limit are taken into account. In Sec. VIII, we summarize our findings and indicate some possible future directions. The 2HDM formalism employed in this paper is reviewed and summarized in Appendix A.

II. C AND P SYMMETRIES IN A GAUGE THEORY OF SPIN-0 AND SPIN-1 FIELDS

Consider a theory of scalar fields and gauge fields. The scalar fields transform locally and nontrivially under a gauge group G. In our analysis, we assume that the gauge theory Lagrangian is renormalizable (i.e., terms of dimension 5 or greater are excluded). We shall allow for all possible terms in the Lagrangian of dimension 4 or less, consistent with the gauge symmetry.

It is well known that if the scalar self-interactions are turned off, then all kinetic energy terms (where derivatives are replaced by covariant derivatives) and mass terms of the Lagrangian separately conserve C, P, and T. When scalar self-interactions are included, CP-violating interaction terms can arise.[4]

Moreover, we assert that, even in the presence of scalar self-interactions, the theory automatically conserves parity. That is, in all scattering processes, any parity-violating observable must vanish. To prove this statement, note that

[4]One further potential source of CP violation can arise via a topological term of the form $\theta F\tilde{F}$, where F is the field strength tensor of the gauge field. However, this is a P-odd, CP-odd term, which is not the focus of this work.

one can consistently choose the P quantum number of $+1$ for all scalar fields and -1 for all gauge fields.[5] One can check that P will be conserved in all interactions. For example, in a vertex with one gauge boson and two scalars, we see that parity is conserved after taking into account the $(-1)^{\ell}$ factor, where $\ell = 1$ is the orbital angular momentum involved in the transition from a spin-1 particle to a pair of spin-0 particles. If the theory exhibits CP violation (or equivalently T violation via the CPT theorem) due to the presence of CP-violating scalar self-interaction terms, then it can be interpreted as C violation.

As another example that illustrates the absence of P-violation, suppose that a scalar mass eigenstate exists that does not possess a definite CP quantum number (which will arise in a theory of a CP-violating scalar sector). In this case, consider the decay of a neutral scalar ϕ to two gauge bosons VV, which can be generated at one loop due to a loop of charged scalars. It is clear that the effective Lagrangian that governs the $\phi \to VV$ decay will be of the form $\mathcal{L}_{\rm eff} = c\phi FF$, where c is a constant that depends on the relevant couplings. Note that the effective operator $\phi F\tilde{F}$ is absent, since it is not possible to generate an $\epsilon_{\mu\nu\alpha\beta}$ at any order of perturbation theory in a renormalizable gauge theory of scalar and gauge fields. Consequently, there cannot be any parity-violating observable associated with the effective ϕVV interaction. Thus, we must again conclude that the presence of CP violation should be interpreted as a violation of C. Indeed, the same argument applies to the analysis of the ZZZ and ZW^+W^- form factor that is generated at one loop due to scalars circulating in the loop, which is discussed in Sec. V.

It is instructive to illustrate these remarks in more detail in a simple setting. Thus, we examine a renormalizable theory of two hypercharge-1 scalar doublets coupled to an $\mathrm{SU}(2) \times \mathrm{U}(1)$ gauge theory. This is the 2HDM with the fermions removed. The theoretical structure of the 2HDM is reviewed in Appendix A, which also establishes our notation.

Consider first the case of a CP-conserving scalar potential and vacuum. In this case, the Higgs basis scalar potential parameters [cf. eq. (A7)] satisfy,

$$\mathrm{Im}(Z_5^* Z_6^2) = \mathrm{Im}(Z_5^* Z_7^2) = \mathrm{Im}(Z_6^* Z_7) = 0. \qquad (6)$$

If eq. (6) is satisfied, then a real Higgs basis exists—that is, one can choose a basis-dependent phase η that appears in the definition of the Higgs basis field $\mathcal{H}_2$ [cf. eq. (A5)] such that all the coefficients Z_i of the scalar potential in the Higgs basis are real.

[5]The choice for -1 for the P quantum number of gauge fields is based on classical arguments. The interaction Lagrangian of the gauge field A_μ is of the form $\mathcal{L} = -j^\mu A_\mu$, and the behavior of the current $j^\mu = \rho u^\mu$ is fixed by parity properties of the 4-velocity vector u^μ.

TABLE I. $J^{\rm PC}$ quantum numbers of the Higgs/Goldstone scalars and gauge bosons of the 2HDM (in the absence of fermions) when the scalar potential and vacuum are CP-conserving [1,61].

Bosonic field	$J^{\rm PC}$	$J^{\rm P}$
γ	1^{--}	
Z	1^{--}	
h, H	0^{++}	
A, G	0^{+-}	
$W^\pm$		1^-
$H^\pm$, $G^\pm$		0^+

In the CP-conserving 2HDM with the fermions removed, C, P, and T are separately conserved, and we can assign in a consistent manner P quantum numbers to all bosonic fields and C quantum numbers to all neutral bosonic fields.[6] In the conventional 2HDM notation, h and H are neutral CP-even Higgs bosons, with $m_h < m_H$; the neutral CP-odd Higgs boson is denoted by A; and $H^\pm$ refers to the charged scalar fields. Working in the R_ξ gauge, one must also include the neutral CP-odd Goldstone field G and the charged Goldstone scalars, $G^\pm$. The C and P assignments were exhibited first in Ref. [61] and are reproduced in Table I (see also Ref. [51]). The quantum numbers presented in Table I have been obtained by examining all possible gauge-invariant bosonic interaction terms of dimension 4 or less. Finally, as discussed above, all scalars are even under parity transformations.

We justify these C and P quantum number assignments with the following arguments. First, the H^+H^- pair with relative orbital angular momentum L has $C = P = (-1)^L$. In light of the existence of the ZH^+H^- coupling, where $L = 1$, it follows that one must assign $J^{PC} = 1^{--}$ for the Z boson. Second, the existence of the hhh_i vertex ($h_i = h, H$) implies the 0^{++} assignment for h, H. Third, the existence of the Zh_ia_j vertex ($a_j = A$, G) justifies the assignment of 0^{+-} for A, G.[7]

[6]This conclusion applies in the case of a generic CP-conserving scalar potential. However, if a $\mathbb{Z}_2$ symmetry is present that is not broken by the vacuum, then one cannot uniquely assign a P quantum number to H and A, although the C quantum numbers of H and A are *relatively* odd. This behavior is associated with the fact that H and A are odd under the $\mathbb{Z}_2$ symmetry. In particular, the $\mathbb{Z}_2$ symmetry removes bosonic vertices of the theory that would otherwise be used to identify the separate C quantum numbers of H and A.

[7]Alternatively, note that the imaginary part of the neutral SM-Higgs doublet is the neutral Goldstone boson, G, which is "eaten" by the Z boson. Like all Goldstone bosons, this field is derivatively coupled and is therefore CP odd. Since we have argued that all scalar bosons are P even and C and P are conserved separately, it follows that the Goldstone boson field G must have $C = -1$.

The absence of certain Higgs couplings such as $W^+W^-a_i$, ZZa_i, Zh_ih_j, and Za_ia_j is in agreement with these C and P assignments.[8] The VVh_i couplings arise from the gauge-covariant kinetic energy terms of the scalar multiplets. Assuming that the vevs are real, no VVa_i term in a CP-conserving theory arises from the covariant derivative terms since a_i derives from the imaginary part of ϕ. In particular, given that the a_i are CP odd, a gauge-invariant interaction with vector bosons must have the form $\epsilon^{\mu\nu\alpha\beta}F_{\mu\nu}F_{\alpha\beta}a_i$, which is a dimension-5 term and is potentially generated at loop level. However, in the bosonic theory, C invariance guarantees that such terms do not arise at loop level.[9] Moreover, the covariant derivative terms do not generate an h_i coupling to a massless vector boson pair (i.e., photons and gluons). These types of couplings only occur at one-loop order through the dimension-5 operator $F_{\mu\nu}F^{\mu\nu}h_i$.

In some cases, the absence of a particular Higgs coupling cannot be attributed to C and P invariance. For example, the $H^+W^-\gamma$ vertex is absent at tree level due to the conservation of the electromagnetic current. The absence of the H^+W^-Z vertex at tree level is a special feature of models with Higgs singlets and doublets and no higher scalar multiplets [1].

III. *P*-EVEN, *CP*-VIOLATING PROCESSES OF EXTENDED HIGGS SECTORS IN THE HIGGS ALIGNMENT LIMIT

As noted earlier, in the absence of fermions, invariance under the parity transformation is always guaranteed. Hence, if the scalar potential of the bosonic Lagrangian violates CP (either explicitly or spontaneously), then any resulting CP-violating phenomena must be associated with a P-conserving C-violating observable. Indeed, an observable that violates both P and CP requires a term in the corresponding scattering or decay matrix element with a Lorentz-structure of the form $\epsilon_{\alpha\beta\gamma\delta}p_1^\alpha p_2^\beta p_3^\gamma p_4^\delta$, with the totally antisymmetric Levi-Civita symbol $\epsilon_{\alpha\beta\gamma\delta}$ and p_i the 4-momenta of the interacting particles. Such a structure can only be generated through interactions with fermions.

In this section, we begin our discussion in the context of the 2HDM and examine how P-even, CP-violating processes of the 2HDM can be observed. We assume that the Higgs alignment limit is exactly realized,[10] which implies the following relations among Higgs basis parameters,

$$Z_6 = 0, \qquad \mathrm{Im}(Z_5 e^{-2i\eta}) = 0, \tag{7}$$

as noted in eq. (A64).

The only potentially complex Higgs basis parameter that remains is Z_7. In the Higgs alignment limit, the bosonic sector of the 2HDM is CP conserving if and only if

$$\mathrm{Im}(Z_5^* Z_7^2) = 0, \tag{8}$$

in light of eq. (6). In particular, eq. (8) is satisfied if and only if

$$\mathrm{Re}(Z_7 e^{-i\eta})\mathrm{Im}(Z_7 e^{-i\eta}) = 0. \tag{9}$$

The neutral scalar squared-mass matrix does not depend on the parameter Z_7. Thus, independently of the value of Z_7, we can regard the neutral scalar squared mass eigenstates as eigenstates of CP, consisting of two CP-even scalars h and H and a CP-odd scalar A, where one of the CP-even states is to be identified with the observed SM-like Higgs boson. If CP violation is present due to $\mathrm{Im}(Z_5^* Z_7^2) \neq 0$, then it is more useful to relabel the neutral states as h_1, h_2, and h_3 (where no mass ordering is implied). One of these three states, which we take by convention to be h_1 (cf. footnote 2), is identified as the SM-like Higgs boson, which in the exact Higgs alignment limit possesses no CP-violating interactions. The remaining two physical neutral scalar states h_2 and h_3 are conventionally defined in the CP-conserving limit following Table II. Without loss of generality, if $Z_7 \neq 0$ and eq. (9) is satisfied, then it is convenient to take $\mathrm{Re}(Z_7 e^{-i\eta}) \neq 0$ and $\mathrm{Im}(Z_7 e^{-i\eta}) = 0$, since the other choice simply interchanges the roles of h_2 and h_3. This is equivalent to declaring h_2 to be CP even and h_3 to be CP odd.

When $\mathrm{Im}(Z_5^* Z_7^2) \neq 0$, then one can regard $\mathrm{Im}(Z_7 e^{-i\eta})$ as a perturbation. In the presence of the perturbation,

TABLE II. CP quantum number of the neutral scalars of the 2HDM in the exact Higgs alignment limit, where $Z_6 = \mathrm{Im}(Z_5 e^{-2i\eta}) = 0$. By definition, the tree-level couplings of h_1 coincide with those of the SM Higgs boson. If $Z_7 = 0$, then the individual quantum numbers of h_2 and h_3 are indeterminate, although the relative sign of the CP quantum numbers of these two states is negative. The CP-even scalar h_1 and the CP-odd Goldstone boson G possess CP-conserving tree-level interactions even in the case of $\mathrm{Re}(Z_7 e^{-i\eta})\mathrm{Im}(Z_7 e^{-i\eta}) \neq 0$, whereas cubic and quartic scalar coupling involving h_2 and h_3 exhibit CP-violating interactions.

Neutral scalar	$\mathrm{Re}(Z_7 e^{-i\eta}) \neq 0$ and $\mathrm{Im}(Z_7 e^{-i\eta}) = 0$	$\mathrm{Re}(Z_7 e^{-i\eta}) = 0$ and $\mathrm{Im}(Z_7 e^{-i\eta}) \neq 0$
h_1	CP even	CP even
h_2	CP even	CP odd
h_3	CP odd	CP even
G	CP odd	CP odd

[8] In the case of $i = j$, the absence of the coupling of the Z to a pair of identical scalars is forbidden by Bose symmetry. For a pair of nonidentical scalars, the coupling is only present if the two scalars have opposite CP quantum numbers as exemplified by the Zh_ia_i vertex.

[9] Since C invariance is broken once we include fermions in the theory, such couplings can be radiatively generated through fermion loops.

[10] This assumption will be relaxed in Sec. VII.

the interactions of h_1 (and G) remain CP conserving in the exact Higgs alignment limit, whereas there exist cubic and quartic scalar interactions involving h_2 and h_3 that violate CP. In particular, the following interactions are the only sources of CP violation due to a nonzero value of $\mathrm{Im}(Z_7 e^{-i\eta})$ in the exact Higgs alignment limit (cf. Table X),

$$\begin{aligned} &h_3h_3h_3, \qquad h_3h_2h_2, \qquad h_3H^+H^-, \\ &h_3h_3h_3h_1, \qquad h_3h_1h_2h_2, \qquad h_3h_1H^+H^-, \end{aligned} \tag{10}$$

as each interaction vertex involves an odd number of would-be CP-odd scalar fields. These interactions guide us to construct scenarios that involve sets of processes whose simultaneous observation would signal the presence of a new scalar source of CP violation. In this section, we shall impose the following three additional requirements: (i) all processes under consideration are unsuppressed in the Higgs alignment limit; (ii) no quartic scalar couplings are involved (due to coupling and phase space suppressions of the corresponding physical processes); and (iii) the dominant contribution to the CP-violating signal is P even. In particular, C-even, CP-violating contributions due to the presence of neutral Higgs-fermion Yukawa couplings are assumed to be either absent or suppressed.[11]

In the 2HDM, we are led to the simultaneous observation of the processes governed by the following bosonic interactions:

$$1.\ h_2H^+H^-, \quad h_3H^+H^-, \quad Zh_2h_3, \tag{11}$$

$$2.\ h_2h_kh_k, \quad h_3H^+H^-, \quad Zh_2h_3, \quad (\text{for } k = 2 \text{ or } 3), \tag{12}$$

$$3.\ h_3h_kh_k, \quad h_2H^+H^-, \quad Zh_2h_3, \quad (\text{for } k = 2 \text{ or } 3), \tag{13}$$

$$4.\ h_2h_kh_k, \quad h_3h_\ell h_\ell, \quad Zh_2h_3, \quad (\text{for } k, \ell = 2 \text{ or } 3). \tag{14}$$

If CP is conserved, then the observation of a Zh_2h_3 interaction would imply that the CP quantum numbers of h_2 and h_3 are relatively odd, whereas the observation of the first two cubic scalar interactions listed above would imply that h_2 and h_3 are both CP even. Consequently, the simultaneous observation of the three interactions in each of the above four cases would unambiguously point to the presence of P-even CP violation.

In a more general extended Higgs sector (e.g., with additional neutral scalar states), the simultaneous observation of the three interactions in each of the following six cases,

$$5.\ h_iH^+H^-, \quad h_jH^+H^- \quad \text{and} \quad Zh_ih_j, \quad (\text{for } i \neq j \text{ and } i, j \neq 1), \tag{15}$$

$$6.\ h_ih_kh_k, \quad h_jH^+H^- \quad \text{and} \quad Zh_ih_j, \quad (\text{for } i \neq j \text{ and } i, j, k \neq 1), \tag{16}$$

$$7.\ h_ih_jh_k, \quad h_kH^+H^- \quad \text{and} \quad Zh_ih_j, \quad (\text{for } i \neq j \neq k \text{ and } i, j, k \neq 1), \tag{17}$$

$$8.\ h_ih_kh_k, \quad h_jh_\ell h_\ell \quad \text{and} \quad Zh_ih_j, \quad (\text{for } i \neq j \text{ and } i, j, k, \ell \neq 1), \tag{18}$$

$$9.\ h_kh_\ell h_\ell, \quad h_ih_jh_k \quad \text{and} \quad Zh_ih_j, \quad (\text{for } i \neq j \neq k \text{ and } i, j, k, \ell \neq 1), \tag{19}$$

$$10.\ h_ih_jZ, \quad h_ih_kZ \quad \text{and} \quad h_jh_kZ, \quad (\text{for } i \neq j \neq k \text{ and } i, j, k, \neq 1), \tag{20}$$

would be a signal of P-even CP violation.

In models with inert scalar doublets in which all physical scalars (with the exception of h_1) are $\mathbb{Z}_2$ odd, the couplings of h_1 are identical to those of the SM Higgs boson. Hence, only the set of couplings exhibited in eq. (20) survive in the inert limit and provide a signature for P-even CP violation.[12] However, the identification of a CP-violating signal in the

[11]The SM fermions can induce a CP-violating $h_iH^+H^-$ interaction that is proportional to the complex CKM phase. However, this effect only enters at the three-loop level and is thus much too small to be observable. Additional CP-violating neutral Higgs-fermion Yukawa couplings can provide sources of P-odd CP violation that would contribute at one loop to the three scalar couplings.

[12]However, inert models based on larger symmetries as in Refs. [28,33,34,62] can yield signals of P-even CP violation in some of the other channels exhibited above.

direct detection of such processes will be quite difficult, since the lightest inert scalar is necessarily stable and thus will result in events with missing energy. On the other hand, the indirect detection of P-even CP violation via loop effects may be viable as discussed in Sec. V.

For a practical application of the scenarios listed in eqs. (11)–(14), we will omit cases that involve the cubic self-interaction of a given scalar. It is noteworthy that the scenario corresponding to eq. (14) involves the discovery of just two neutral states. In the next section, we shall first focus on processes in which h_2 and h_3 can be observed via an s-channel Z exchange. Once h_2 and h_3 are established, one can search for $h_2h_2h_3$ and $h_2h_3h_3$ production (which are also mediated via an s-channel Z exchange). Simultaneous observation of both production channels would signal the presence of P-even CP violation. The other scenarios corresponding to eqs. (11)–(13) also require the observation of a charged Higgs boson. Thus, in the next section, we also examine a suite of processes in which h_2, h_3, and $H^\pm$ can be observed.

For certain scalar mass spectra, it is possible to access all three vertices of a given scenario from one production process. For example, consider h_2h_3 production via s-channel Z exchange. If kinematically accessible, both h_2 and h_3 could have observable branching ratios into H^+H^-, in which case the observation of h_2h_3 production via their respective decays into H^+H^- would yield a simultaneous observation of all three processes listed in eq. (11).

The vertices listed in eqs. (11)–(14) are unsuppressed in the Higgs alignment limit, and none involves quartic scalar couplings. Any contributions of C-even, CP-violating interactions via the Yukawa couplings are loop suppressed. Thus, to a good approximation, the simultaneous observation of the three processes in any of the scenarios listed in eqs. (11)–(14) would constitute an unambiguous signal of P-even CP violation.

The detection of P-even, CP-violating signals at colliders requires the simultaneous observation of processes typically governed by three distinct bosonic interactions. In some cases, the relevant observable involves an on-shell two-body scalar. In other cases, the relevant bosonic interaction can only be probed when at least one of the bosonic states is off shell. Typically, the on-shell decay processes are the easiest to observe and interpret, although the kinematic availability of such processes will depend on a favorable spectrum of scalar masses. A more comprehensive search for P-even, CP-violating signals will require an experimental probe of bosonic interactions involving off-shell scalars. Such processes will require higher statistical data samples, subtraction of backgrounds, and more sophisticated methods to interpret the relevant signals.

IV. OBSERVATION OF *P*-EVEN, *CP*-VIOLATING SCALAR PROCESSES AT LEPTON COLLIDERS

We begin with the assumption that the neutral scalars (beyond the SM-like h_1) and the charged scalars of the extended Higgs sector have been discovered in future runs of the LHC and/or at some future lepton collider. For example, neutral heavy scalars can typically be produced via gluon-gluon fusion and discovered through their decays into heavy fermion pairs at the LHC over a significant part of the scalar sector parameter space (e.g., see Refs. [63,64]). At an e^+e^- collider operating at a center of mass (CM) energy of 500 GeV to 1 TeV, new scalars of an extended Higgs sector can be discovered, as shown in Ref. [65], if kinematically accessible and if their main decay modes can be probed (with decays to b-quarks typically the most relevant for scalar masses below $2m_t$). For example, the process $e^+e^- \to HA$ was examined in Ref. [65] in the framework of the minimal supersymmetric extension of the Standard Model (MSSM) close to the decoupling limit (where the scalars H and A are roughly mass degenerate), and the cross section reaches its maximum value. The authors concluded that for a linear collider with $\sqrt{s} = 800$ GeV with an integrated luminosity of 500 fb^{-1}, it would be possible to observe $e^+e^- \to HA$ (at a level of 5σ statistical significance) for scalar masses of around 385 GeV. In this case, the tree-level cross section $\sigma(e^+e^- \to HA)$ is about 2 fb, which yields 1000 signal events before cuts.

Higher energy e^+e^- colliders with $\sqrt{s} \geq 1$ TeV can significantly extend the discovery reach of heavy scalars. For example, Ref. [66] considered the production of a heavy scalar H via the process $e^+e^- \to H\nu\bar{\nu}$ with the subsequent decay $H \to hh \to 4b$. This study was performed for the proposed Compact Linear Collider (CLIC) with a CM energy of 3 TeV assuming an integrated luminosity of 2 ab^{-1}. The authors concluded that the sensitivity for discovery in the mass range 250 GeV $\leq m_H \leq 1$ TeV provides up to 2 orders of magnitude improvement in sensitivity compared to the discovery potential at the High Luminosity (HL) LHC.

The unambiguous observation P-even CP-violating phenomena via any one of the four sets of three interaction vertices exhibited in eqs. (11)–(14) at the LHC of is a challenging task. In contrast, at a lepton or photon collider, the corresponding backgrounds that must be subtracted to reveal the signal are significantly easier to handle. The corresponding signals at a lepton or photon collider provide direct access to the interaction vertices exhibited in eqs. (11)–(14) at tree level that can be directly identified as P-even and CP violating (once the three interaction vertices of a given set are confirmed). Moreover, potential P-odd, CP-violating effects that would involve scalar couplings to fermions only arise at the one-loop level and are hence

TABLE III. Accelerators used in the analysis with different CM energies proposed and the corresponding total integrated luminosity after the completion of a multiyear program (typically of order 10 years).

Accelerator	$\sqrt{s}$ (TeV)	Integrated luminosity (ab^{-1})
CLIC	1.5	2.5
CLIC	3	5
Muon collider	3	1
Muon collider	10	10
Muon collider	14	20

subdominant. Of course, the Yukawa couplings will enter when considering the decays of the produced neutral and charged Higgs bosons, which we shall address at the end of this section.

A. Discovery potential at future lepton (and photon) colliders

Consider the discovery potential of final states related to the *P*-even, *CP*-violating observables at future lepton colliders listed in Table III. CLIC [67] is an electron-positron collider that has been proposed to run at CM energies of 1.5 and 3 TeV with total integrated luminosities of 2.5 and 5 ab^{-1}, respectively, after the completion of a multiyear program (typically of order 10 years). We also consider the possibility of a muon collider [68] with CM energies of 3, 10, and 14 TeV and with total integrated luminosities of 1, 10, and 20 ab^{-1}, respectively. In addition, we shall show results for a photon-photon collider of CM energies of 1 and 2 TeV that could be achieved via the Compton backscattering of laser light on high energy electrons at CLIC [69]. Other lepton colliders now under development such as the Circular Electron Positron Collider in China [70] ($\sqrt{s}_{\max} \sim 250$ GeV), the International Linear Collider in Japan [71] ($\sqrt{s}_{\max} \sim 250$ GeV), and the FCC-ee at CERN ($\sqrt{s}_{\max} \sim 365$ GeV) [72] have energies well below the production threshold of our final states and thus are not considered here.

Although lepton colliders provide a very clean environment for the final states of the processes under consideration, a proper analysis would still have to take into account both the efficiencies and the main background processes. Nevertheless, having assumed above that the scalars of the extended Higgs sector have already been discovered, either at the HL-LHC or at an e^+e^- collider of sufficient CM energy, one can consider smaller samples of signal events (compared, say, to the 1000 events before cuts employed in Ref. [65]) in searches for *P*-even *CP*-violating phenomena using di-Higgs and tri-Higgs final states via the processes specified in eqs. (11)–(14). In this work, we are considering lepton collider luminosities that are roughly 1 order of magnitude larger than employed in earlier studies that focused on lower energy colliders. Thus, to ensure at least 100 events before cuts, signals of interest should have cross sections that are above 10–100 ab.

B. Coupling parameters that govern the three-scalar interactions

As previously indicated, the observed SM-like Higgs boson is denoted by $h_1(125)$. In the context of the 2HDM, one needs to simultaneously detect the other two scalars h_2 and h_3 either in production or decay processes involving the interaction vertices Zh_2h_3, $H^+H^-h_2$ (or alternatively $h_3h_3h_2$), and $H^+H^-h_3$ (or alternatively $h_2h_2h_3$). In principle, h_2 and h_3 can be either heavier or lighter than the SM-like Higgs boson. As we will be working in the exact Higgs alignment limit, the tree-level couplings λ_{ZZh_2} and λ_{ZZh_3} as well as $\lambda_{Zh_2h_1}$ and $\lambda_{Zh_3h_1}$ vanish, precluding the possibility of using a combination of these decays to signal *CP* violation as discussed in Refs. [50,52,53]. In the exact Higgs alignment limit, the interaction vertices that contribute to the *P*-even, *CP*-violating observables corresponding to eqs. (11)–(14) can be obtained from Table X of Appendix A,

$$\lambda_{H^+H^-h_1} = vZ_3, \qquad \lambda_{H^+H^-h_2} = \lambda_{h_3h_3h_2} = v\mathrm{Re}\bar{Z}_7,$$
$$\lambda_{H^+H^-h_3} = \lambda_{h_2h_2h_3} = -v\mathrm{Im}\bar{Z}_7, \tag{21}$$

where $\bar{Z}_7 \equiv Z_7 e^{-i\eta}$ is defined in eq. (A39). Thus, the production rate for each process governed by the $\varphi^*\varphi h_i$ interaction vertices, where $\varphi = H^+$ or h_j ($j \neq i$, $j \neq 1$), is proportional to Λ_i^2 defined by

$$\Lambda_1 \equiv \lambda_{H^+H^-h_1}/v, \qquad \Lambda_2 \equiv \lambda_{H^+H^-h_2}/v = \lambda_{h_3h_3h_2}/v,$$
$$\Lambda_3 \equiv -\lambda_{H^+H^-h_3}/v = -\lambda_{h_2h_2h_3}/v. \tag{22}$$

In particular,

$$\Lambda_1 = Z_3, \qquad \Lambda_2 = \mathrm{Re}\bar{Z}_7, \qquad \Lambda_3 = \mathrm{Im}\bar{Z}_7. \tag{23}$$

The detection of scalars in decay processes with fermionic final states depends on the Yukawa couplings for which there is some freedom in the 2HDM. In order to maximize this freedom while avoiding tree-level flavor changing neutral currents, we shall employ the Yukawa sector of the flavor-aligned 2HDM (A2HDM) [73] as a benchmark in the Higgs alignment limit [cf. eq. (A71)]. With this choice, the Yukawa couplings are independent of the gauge couplings and of the parameters of the scalar potential, which in turn weakens the constraints on the scalar masses.

C. Allowed mass range for non-SM Higgs states of the 2HDM

The processes that we propose as probes of *P*-even *CP* violation involve the production of neutral Higgs bosons [e.g., h_2 and h_3, but excluding the $h_1(125)$] and charged

Higgs bosons. Experimental searches for these scalar states have already yielded some constraints on their masses and couplings. The production of charged Higgs bosons at the LHC is governed mainly by the Yukawa interactions via $pp \to tbH^{\pm}$ with subsequent decay channels, $H^{\pm} \to tb$, $H^{\pm} \to \tau\nu$, and $H^{\pm} \to cs$. Charged Higgs bosons can also be produced via scalar or gauge boson exchange, as in the s-channel (Drell-Yan type) processes $\bar{u}(\bar{c})d(s,b) \to W^- \to H^- h_i$ (and its conjugate process) and also via $\bar{f}f \to \gamma(Z) \to H^+H^-$.[13]

The LHC searches performed so far rely on the charged Higgs couplings to fermions. For example, in a CP-conserving 2HDM with type-I Yukawa couplings in the exact Higgs alignment limit, the Yukawa coupling of h_1 coincides with that of the SM, whereas the Yukawa couplings of all other scalar states (both neutral and charged) are proportional to a common factor of $1/\tan\beta$. That is, the couplings of the charged Higgs boson to fermions are suppressed at large $\tan\beta \gtrsim 10$, in which case a charged Higgs mass of the order of 100 GeV [75–77] is still allowed. Indeed, other constraints on the parameter space, such as those derived from $pp \to A \to Zh_i$ searches, are also weakened if $\tan\beta$ is large. In order to circumvent the smallness of the Yukawa couplings, the authors of Ref. [76] proposed employing the processes $\bar{u}(\bar{c})d(s,b) \to W^- \to H^- h_i \to W^- h_i h_j (i,j = 2,3)$ to search for charged Higgs bosons at the LHC. The corresponding production rates only depend on the Yukawa couplings in the decays of the neutral scalars. The cross sections can reach a few hundred femtobarns if both scalars are relatively light (i.e., not much heavier than 100 GeV).

The Yukawa sector of the A2HDM is less constrained than that of a type-I 2HDM in light of the recent global fit of Ref. [78] (which assumed no new sources of CP violation beyond the CKM phase). Hence, light charged Higgs bosons are also not excluded in the A2HDM. As for the neutral scalars h_2 and h_3, these scalars do not couple to gauge bosons in the exact Higgs alignment limit. Their couplings to fermions can also be significantly smaller than those of the SM-like Higgs boson h_1. In particular, the couplings of h_2 and h_3 to top quarks are suppressed by $1/\tan\beta$ in the 2HDM with type-I, -II, -X, or -Y Yukawa couplings when $\tan\beta \gg 1$. Therefore, it is quite likely that h_2 and h_3 with masses as low as 100 GeV could have so far evaded detection in a non-negligible region of the 2HDM parameter space.

D. Cross sections for P-even, CP-violating scalar processes

The cross sections presented in this section are calculated using SARAH4.14.4 [79,80] to generate the Feynman rules for the model and MADGRAPH5_AMC@NLO [81] to evaluate the cross section for the different scenarios. The Equivalent Photon Approximation is used [82,83] by MADGRAPH5 when calculating the cross sections $\ell^+\ell^- \to \ell^+\ell^- H^+H^- h_i$ (see also the recent work dedicated to muon colliders [84]).

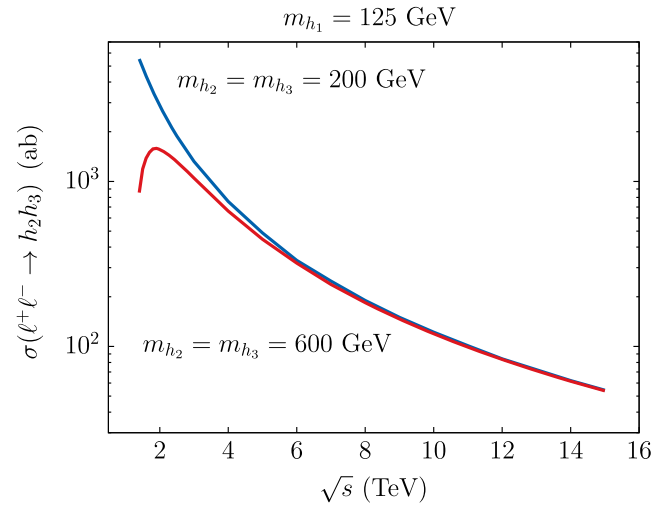

FIG. 1. $\sigma(\ell^+\ell^- \to h_2h_3)$ as a function of the CM energy for $m_{h_2} = m_{h_3} = 200$ GeV and $m_{h_2} = m_{h_3} = 600$ GeV.

Let us first consider the production process $\ell^+\ell^- \to h_2h_3$, for which the main contribution comes from a tree-level s-channel process with Z boson exchange. In the Higgs alignment limit, this is purely an electroweak process, and the number of Higgs bosons produced depends only on their masses. In Fig. 1, we show the total cross section $\sigma(\ell^+\ell^- \to h_2h_3)$ as a function of the CM energy for $m_{h_2} = m_{h_3} = 200$ GeV and for $m_{h_2} = m_{h_3} = 600$ GeV. As expected, the cross section falls with the CM energy but is still above 1000 ab for both scenarios for $\sqrt{s} = 3$ TeV. This means that there is a good chance of producing and detecting the two scalars even if they are heavy. For even higher CM energies, the number of events will decrease, but the dependence on the masses of the scalars will become milder.

These scalars still have to be detected in some particular final state. In the exact Higgs alignment limit, h_2 and h_3 cannot decay to gauge bosons. To simplify the discussion of the possible final states, let us assume $m_{h_2} \leq m_{h_3}$. The most relevant h_2 and h_3 decay modes (if kinematically allowed) are $h_3 \to h_2Z$, $h_3 \to h_2h_2$, $h_{2,3} \to H^{\pm}W^{\mp}$, $h_{2,3} \to H^+H^-$, $h_{2,3} \to \bar{t}t$, $h_{2,3} \to \bar{b}b$, and $h_{2,3} \to \tau^+\tau^-$. Because the couplings of h_2 and h_3 to other scalars can be large enough to allow the decays to charged scalars to be dominant, this process alone could signal P-even CP violation in the exact Higgs alignment limit (e.g., by considering $h_3 \to h_2h_2$ and $h_2 \to H^+H^-$). Clearly, all the masses would have to be fully reconstructed via the hadronic decays of the charged Higgs boson, which can be carried out at a lepton collider (where the cross sections for

[13]See, e.g., Ref. [74] for a list of the main charged Higgs production processes at the LHC.

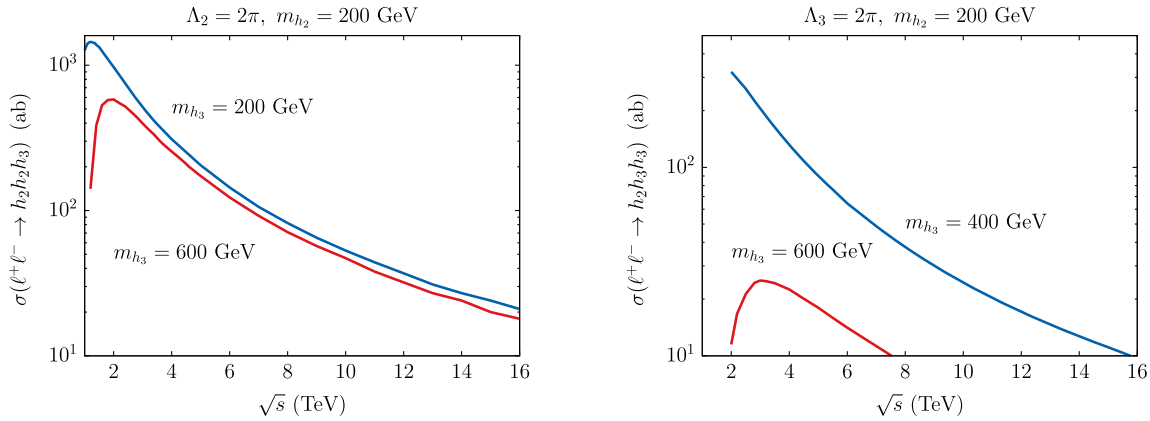

FIG. 2. $\sigma(\ell^+\ell^- \to h_2h_2h_3)$ (left) and $\sigma(\ell^+\ell^- \to h_2h_3h_3)$ (right) as a function of the CM energy, with $m_{h_2} = 200$ GeV.

the relevant background processes are of the same order of magnitude as the signal process).

If the two-body decays of h_2 and h_3 into bosonic final states are kinematically forbidden, then it is necessary to consider separately the three production processes governed by one of the sets of bosonic interactions listed in eqs. (11)–(14). This strategy has the advantage of being constrained only by the collider energy but the disadvantage of requiring the observation of three-body processes with smaller cross sections.

We begin with the s-channel three-body process with the exchange of a Z boson. In Fig. 2, we fix the value of $m_{h_2} = 200$ GeV and plot the total cross sections for $\ell^+\ell^- \to h_ih_jh_j$ (for $i \neq j = 2, 3$) as a function of the CM energy. In the left panel of Fig. 2, we exhibit $\sigma(\ell^+\ell^- \to h_2h_2h_3)$ with $\Lambda_2 = 2\pi$ for two choices of $m_{h_3} = 200$ and 600 GeV, and in the right panel, we exhibit $\sigma(\ell^+\ell^- \to h_2h_3h_3)$ with $\Lambda_3 = 2\pi$ for two choices of $m_{h_3} = 400$ and 600 GeV. The cross section for $\ell^+\ell^- \to h_2h_2h_3$ is dominated by the value Λ_2 because of the relation $\lambda_{h_2h_2h_2} = 3\lambda_{h_3h_3h_2} = \Lambda_2/v$ (cf. Table X). All diagrams except for the ones with two Zh_2h_3 vertices are proportional to Λ_2, and in the region relevant for our analysis where $\Lambda_2 > 1$, all other contributions are negligible. The same can be said for the relation between $\sigma(\ell^+\ell^- \to h_3h_3h_2)$ and the value of Λ_3 because $\lambda_{h_3h_3h_3} = 3\lambda_{h_2h_2h_3} = -\Lambda_3/v$ (cf. Table X). The results shown in Fig. 2 suggest that if the masses of h_2 and h_3 are not significantly heavier than the scale of electroweak symmetry breaking, then the observation of $\ell^+\ell^- \to h_ih_jh_j$ will provide an opportunity for detecting evidence for P-even CP violation (if present), if the CM energy of the lepton collider is in the range of 1–3 TeV.

Consider next the t-channel processes, which are dominated by $\gamma\gamma$ fusion with a cross section that is proportional to $\ln^2(s/m_\ell^2)$. There are also Z fusion diagrams contributing, but the corresponding cross sections are proportional to $\ln^2(s/m_Z^2)$ [85] and are thus subdominant. In light of eq. (22), the cross section for any final state of the type $H^+H^-h_i$ (for $i = 1, 2, 3$) is proportional to Λ_i^2. That is, by choosing $\Lambda_1 = \Lambda_2 = \Lambda_3 = 2\pi$, the cross sections exhibited in this section are applicable to any of the neutral scalars.

In Figs. 3–7, we present cross sections for the production of $H^+H^-h_i$ final states. In order to confirm the existence of P-even, CP-violating phenomena (if present), we shall focus primarily on processes that include h_2 or h_3 in the final state. If such channels are detected, then it will also be possible to observe the $H^+H^-h_1$ final state. Note that the production cross section for h_1 is proportional to the factor Λ_1, which provides us with a benchmark cross section for a final state with at least one known particle.

In Fig. 3, we plot the cross sections, $\sigma(e^+e^- \to e^+e^-H^+H^-h_i)$, $\sigma(\mu^+\mu^- \to \mu^+\mu^-H^+H^-h_i)$, and $\sigma(\ell^+\ell^- \to H^+H^-h_i)$, as a function of the CM energy. In the left panel, we have chosen a neutral scalar boson with $m_{h_i} = 125$ GeV and a charged Higgs boson with $m_{H^\pm} = 150$ GeV. For $i = 1$, the corresponding plot refers to the production of the SM-like Higgs boson. For $i = 2$ and 3, the same plot refers to the production of the scalar h_i of mass 125 GeV, assuming that $\Lambda_i = 2\pi$. Although we do not expect either h_2 and h_3 to be (approximately) degenerate in mass with h_1,[14] we exhibit these figures to provide the reader with a sense of how large the cross sections of interest may be. In the right panel, the masses are chosen to be $m_{h_i} = m_{H^\pm} = 300$ GeV. The parameters of the potential are $\Lambda_i = 2\pi$. As expected, the first two cross sections that occur mainly via $\gamma\gamma$ fusion grow with the collider energy as $\ln^2(s/m_\ell^2)$. Taking into account only the leading term in the Equivalent Photon Approximation, which scales as $\ln^2(s/m_\ell^2)$, the ratio of the electron to muon cross section yields 2.5 for $\sqrt{s} = 1$ TeV and 2.1 for $\sqrt{s} = 10$ TeV. The t-channel and s-channel cross sections are complementary

[14]Indeed, this possibility of an approximate mass degeneracy is either excluded based on present LHC Higgs data or will be excluded by the time the higher energy lepton colliders are operational [86–89].

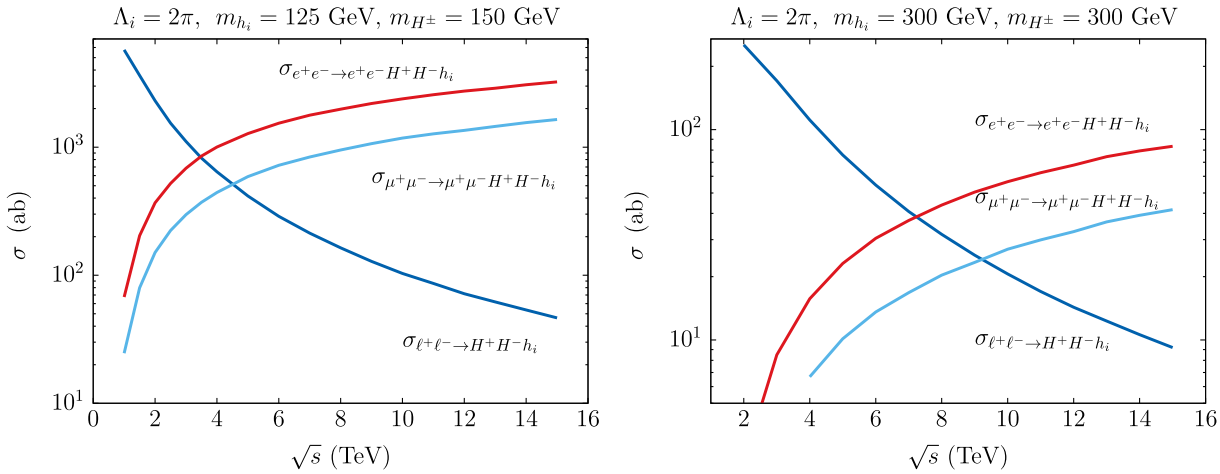

FIG. 3. $\sigma(e^+e^- \to e^+e^-H^+H^-h_i)$, $\sigma(\mu^+\mu^- \to \mu^+\mu^-H^+H^-h_i)$, and $\sigma(\ell^+\ell^- \to H^+H^-h_i)$ as a function of the CM energy. In the left panel, $m_{h_i} = 125$ GeV and $m_{H^\pm} = 150$ GeV, and in the right panel, $m_{h_i} = m_{H^\pm} = 300$ GeV. The scalar potential parameters are chosen such that $\Lambda_i = 2\pi$.

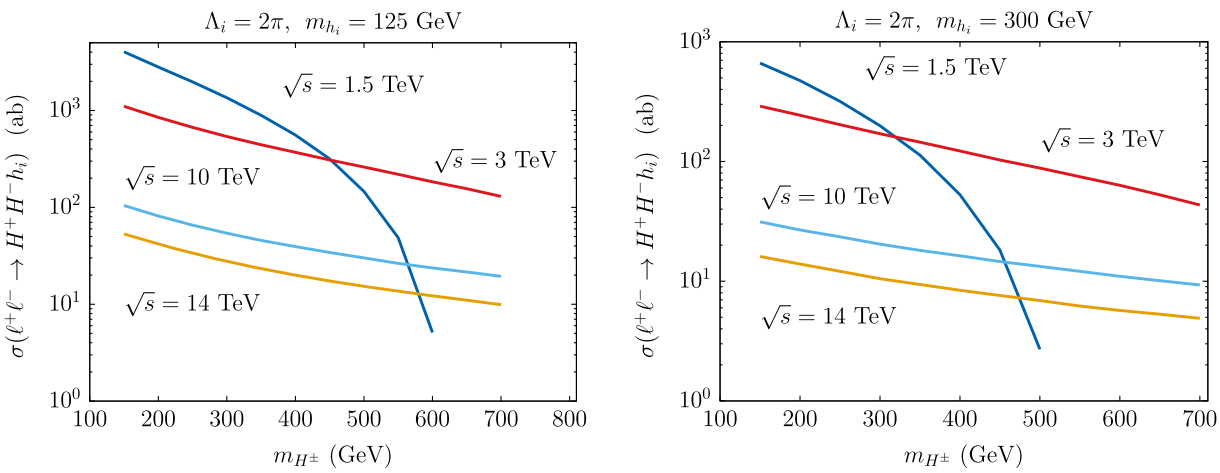

FIG. 4. $\sigma(\ell^+\ell^- \to H^+H^-h_i)$ as a function of the charged Higgs mass for four CM energies of $\sqrt{s} = 1.5$, 3, 10 and 14 TeV. In the left panel $m_{h_i} = 125$ GeV, and in the right panel $m_{h_i} = 300$ GeV. The scalar potential parameters are chosen such that $\Lambda_i = 2\pi$.

to each other, giving us access to the final state $H^+H^-h_i$ at both the low and high energy ends. Note that, even with the coupling constants as large as $\Lambda_i = 2\pi$, the maximum value for the s-channel cross section for $m_{h_i} = m_{H^\pm} = 300$ GeV is roughly 200 ab, and the corresponding maximum value for $\gamma\gamma$ fusion cross section is below 100 ab for e^+e^- and below 50 ab for $\mu^+\mu^-$ processes. Hence, if both the neutral and the charged Higgs bosons are simultaneously heavy, it is unlikely that we will be able to detect these final sates. In the next plots, we present in more detail how the different cross sections vary with the scalar masses.

In Fig. 4, we exhibit the cross section $\sigma(\ell^+\ell^- \to H^+H^-h_i)$ as a function of the charged Higgs mass for four CM energies of $\sqrt{s} = 1.5$, 3, 10, and 14 TeV. This covers the energy ranges of both CLIC and the muon collider. Note that for the s channel, the e^+e^- and $\mu^+\mu^-$ cross sections have the same values. In the left panel, we have set $m_{h_i} = 125$ GeV, and in the right panel, $m_{h_i} = 300$ GeV. Clearly, there is a wide range of charged Higgs masses that can be probed for all collider energies.

In Fig. 5, we present the cross section $\sigma(e^+e^- \to e^+e^-H^+H^-h_i)$ via $\gamma\gamma$ fusion at CLIC as a function of the charged Higgs mass in the left panel and as a function of the neutral Higgs mass in the right panel, for two CM energies of $\sqrt{s} = 1.5$ and 3 TeV. Again, we choose $\Lambda_i = 2\pi$. We shall insist that the corresponding cross sections must exceed (roughly) 10 ab in order that the SM-like Higgs boson can be detected in association with a charged Higgs boson pair at CLIC. In light of the results exhibited in the left panel of Fig. 5, it follows that $m_{H^\pm}$ can be at most 300 GeV for $\sqrt{s} = 1.5$ TeV and 500 GeV for $\sqrt{s} = 3$ TeV. This behavior is expected because at these CM energy ranges the s-channel production process provides the dominant contribution. In the right panel of

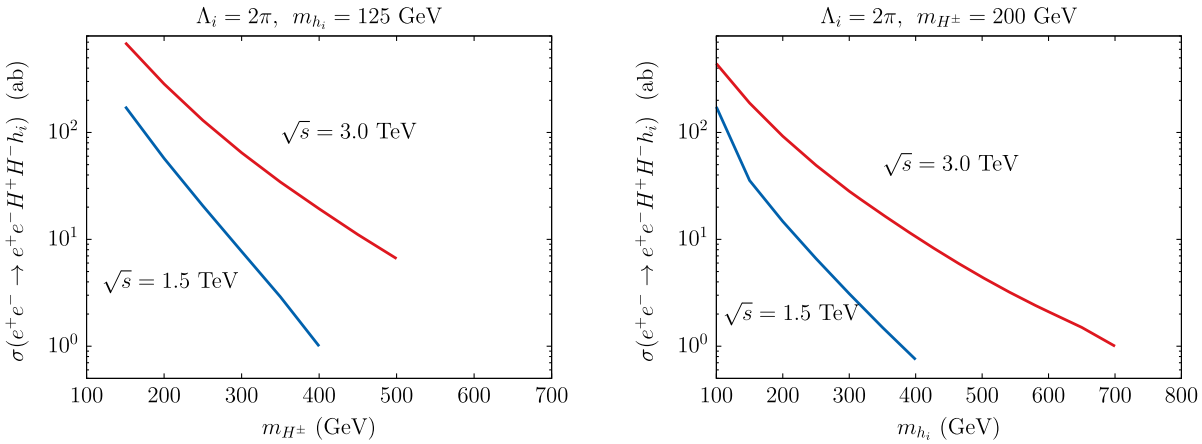

FIG. 5. $\sigma(e^+e^- \to e^+e^-H^+H^-h_i)$ via $\gamma\gamma$ fusion as a function of the charged Higgs mass (left) and of the neutral Higgs mass (right) for two CM energies of $\sqrt{s} = 1.5$ TeV and $\sqrt{s} = 3$ TeV. The scalar potential parameters are chosen such that $\Lambda_i = 2\pi$.

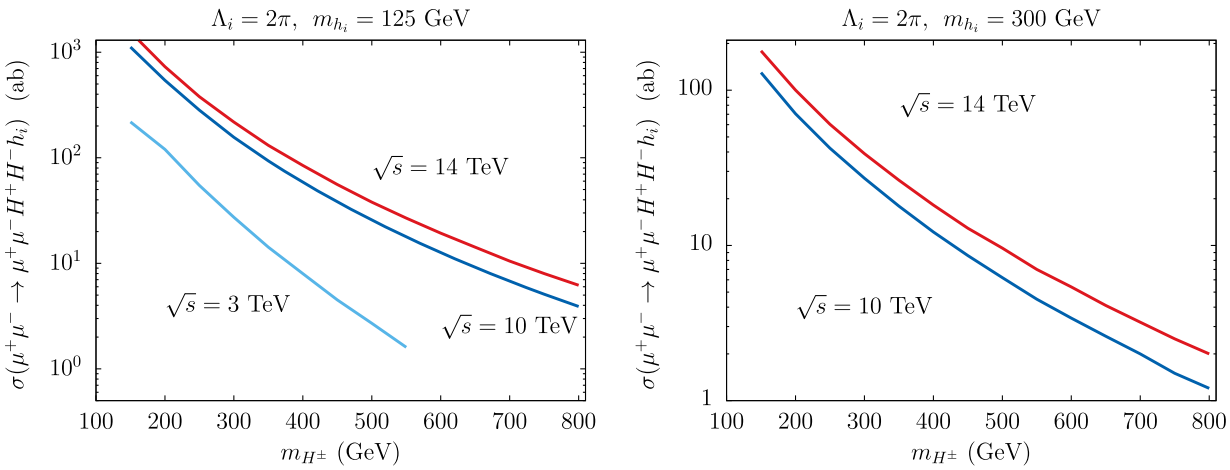

FIG. 6. $\sigma(\mu^+\mu^- \to \mu^+\mu^-H^+H^-h_i)$ as a function of the charged Higgs mass for three CM energies of $\sqrt{s} = 3$, 10, and 14 TeV. In the left panel, $m_{h_i} = 125$ GeV, and in the right panel, $m_{h_i} = 300$ GeV. The scalar potential parameters are chosen such that $\Lambda_i = 2\pi$.

Fig. 5, if the charged scalar has a mass of 200 GeV, then the neutral scalar masses need to be less than about 200 GeV for $\sqrt{s} = 1.5$ TeV and less than about 400 GeV for $\sqrt{s} = 3$ TeV.

In Fig. 6, we show the cross section $\sigma(\mu^+\mu^- \to \mu^+\mu^-H^+H^-h_i)$ as a function of the charged Higgs mass for three CM energies of $\sqrt{s} = 3$, 10, and 14 TeV. In the left panel, $m_{h_i} = 125$ GeV, and in the right panel, $m_{h_i} = 300$ GeV, and the relevant parameters of the potential are set to $\Lambda_i = 2\pi$. Again, we see that a large number of events will be produced if one of the Higgs bosons is light, but detection will be difficult if both the neutral and the charged Higgs bosons are heavy.

There are currently no plans to alter the CLIC design to permit it to run in a $\gamma\gamma$ collider mode. Nevertheless, it is instructive to have some measure of what to expect at such a facility. Here, we assume following Ref. [69] that the $\gamma\gamma$ CM energy is approximately 80% of the e^+e^- CM energy, i.e., roughly 1.25 and 2.5 TeV, with a luminosity of the order of 10% of the CLIC design luminosity.[15] We show in Fig. 7 the cross section for the scattering of two on-shell photons,

[15]The $\gamma\gamma$ collider luminosity assumed in Ref. [69] may be somewhat optimistic. A more recent study of multi-TeV $\gamma\gamma$ colliders carried out in Ref. [90] examines the possibility of employing a free electron laser in the construction of a high luminosity $\gamma\gamma$ collider with a CM energy in the multi-TeV regime. For example, Table 4 of Ref. [90] imagines an e^+e^- collider with $\sqrt{s} = 3$ TeV, which yields $\gamma\gamma$ collisions with $E_\gamma = 1.38$ TeV and a luminosity of $L_{\gamma\gamma} \leq 0.06 L_{ee}$, corresponding to a $\gamma\gamma$ collider with a slightly higher CM energy and a slightly lower luminosity, as compared to $\sqrt{s_{\gamma\gamma}} = 2.5$ TeV and $L_{\gamma\gamma} = 0.1 L_{ee}$ discussed in Ref. [69]. An alternative approach has been investigated in Ref. [91], which examines a $\gamma\gamma$ collider based on an e^-e^- linear collider with $\sqrt{s} = 2$ TeV. These authors claim a maximal photon energy of $E_\gamma = 0.95$ TeV but with a luminosity of $L_{\gamma\gamma} = 0.02 L_{ee}$. Such a collider would yield an integrated luminosity of roughly 0.1 ab^{-1} over a 10 year program, which would be insufficient to study *P*-even, *CP*-violating phenomena over most of the scalar mass range of interest. We thank the referee for alerting us to these two references cited above.

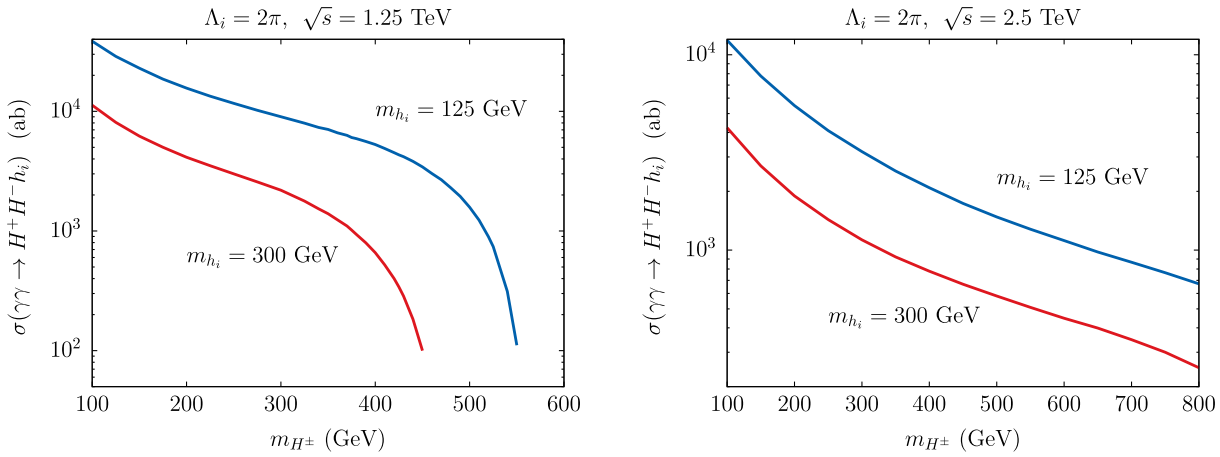

FIG. 7. The cross section $\sigma(\gamma\gamma \to H^+H^-h_i)$ as a function of the charged Higgs mass for two CM energies, $\sqrt{s} = 1.25$ TeV (left panel) and $\sqrt{s} = 2.5$ TeV (right panel), for two values for the neutral Higgs masses, $m_{h_i} = 125$ GeV and $m_{h_i} = 300$ GeV. The scalar potential parameters are chosen such that $\Lambda_i = 2\pi$.

$\sigma(\gamma\gamma \to H^+H^-h_i)$, as a function of the charged Higgs mass for two CM energies $\sqrt{s} = 1.25$ TeV (left panel) and $\sqrt{s} = 2.5$ TeV (right panel), for two values for the neutral Higgs masses, $m_{h_i} = 125$ GeV and $m_{h_i} = 300$ GeV. In light of eq. (22), it follows that $\sigma(\gamma\gamma \to H^+H^-h_i)$ is proportional to Λ_i^2. The cross sections shown in the plots for $\gamma\gamma$ fusion are all above 100 ab, and with the planned luminosity for CLIC, the $\gamma\gamma$ collider would provide a larger number of signal events than the corresponding signals anticipated at the lepton colliders discussed in this section. However, the CM energy of the $\gamma\gamma$ collider will restrict the observable scalar masses accessible in the production of $H^+H^-h_i$ to no more than a few hundred GeV.

In light of our considerations of the $\gamma\gamma$ fusion processes at lepton colliders above, a brief comment on $\gamma\gamma$ physics at the LHC is warranted. The ATLAS Collaboration has reported [92] the observation of photon-induced W^+W^- production in pp collisions at $\sqrt{s} = 13$ TeV with 139 fb^{-1} of data in the process $\gamma\gamma \to W^+W^- \to e^\pm\mu^\mp + \not{E}_T$, with an observed cross section of $3.13 \pm 0.31\,(\text{stat}) \pm 0.28\,(\text{syst})$ fb. In light of this measurement, it is of interest to consider whether $\gamma\gamma \to H^+H^-$ is within the reach of the LHC program. The cross section for $pp \to ppH^+H^-$ via photon fusion was calculated in Ref. [93] and shown to be about 0.1 fb for a charged Higgs mass of 150 GeV at $\sqrt{s} = 14$ TeV. One must also account for the charged Higgs boson decay channels, while contending with a significant $\gamma\gamma \to W^+W^-$ irreducible background with a much larger cross section. Therefore, although not impossible, it will be very difficult to detect charged Higgs bosons produced via $\gamma\gamma$ fusion at the LHC. If in addition, one demands that a neutral Higgs boson is emitted from one of the final state (virtual) charged Higgs bosons, then the resulting $\gamma\gamma \to H^+H^-h_i$ cross section will be too small to be detected at the LHC (even with the anticipated 2 ab dataset at the HL-LHC).

Finally, we discuss the detection prospects of the final states produced by the processes analyzed in this section. To reiterate, we are assuming the exact Higgs alignment limit where the tree-level properties of h_1 coincide precisely with those of the observed SM-like Higgs boson. In the A2HDM, the couplings of the up- and down-type quarks to h_2, h_3, and $H^\pm$ are exhibited in eq. (A54). In the Higgs alignment limit, the couplings to the neutral scalars, h_2 and h_3, reduce to the form shown in eq. (A71) [whereas the corresponding couplings to $H^\pm$ shown in eq. (A54) are unchanged]. The corresponding couplings of the leptons are obtained by replacing the down-type (up-type) quark fields with the corresponding charged lepton (neutrino) fields, replacing M_D by the diagonal lepton mass matrix and replacing M_U with the zero matrix. The charged Higgs boson can be detected via one of its decay channels: $W^\pm h_2$, $W^\pm h_3$, or a fermion pair, as discussed below.[16]

Considering that all Yukawa couplings can be independently chosen in flavor-aligned extended Higgs sectors, one must take into account all final states with quark pairs of different generations. Assuming a good b and c tagging efficiency and denoting light quark (u, d, s) jets collectively by j, the final states resulting from the $H^\pm$ decay to a fermion pair will be combinations of tb (or tj), cb (or cj or jb), or $\tau^\pm$ and missing transverse energy. At a lepton collider, one can employ the hadronic decay modes of the charged Higgs boson to reconstruct its mass. At tree level, the other important decay channels are $H^\pm \to W^\pm h_2$ and $H^\pm \to W^\pm h_3$ with rates proportional to square of the $\text{SU}(2)_L$ electroweak coupling, g^2. At one loop, the subdominant decay mode $H^\pm \to W^\pm\gamma$ could eventually be utilized if a sufficiently large data sample were available.

[16]Note that the $H^\mp W^\pm h_1$ coupling vanishes in the Higgs alignment limit.

The neutral Higgs bosons h_2 and h_3 do not couple to pairs of gauge bosons in the exact Higgs alignment limit and hence do not decay (at tree level) to W^+W^- and ZZ. If kinematically allowed, the decays $h_2 \to W^\pm H^\mp$, Zh_3 and $h_3 \to W^\pm H^\mp$, Zh_2 have to be considered particularly because their rates are proportional to g^2. The tree-level decay rates of the neutral scalars h_2 and h_3 to fermion pairs will be dominated by third-generation final states, $t\bar{t}$, $b\bar{b}$, and $\tau^+\tau^-$. In addition, the one-loop neutral Higgs decay modes to a pair of gluons may also be competitive. The subdominant one-loop neutral Higgs decay modes to $\gamma\gamma$, $Z\gamma$ could eventually be utilized if a sufficiently large data sample were available.

V. *P*-EVEN, *CP*-VIOLATING SIGNALS VIA LOOP EFFECTS

An indirect way to examine the set of Higgs couplings exhibited in eq. (20) that yield P-even, CP-violating signals considered in Secs. III and IV is to probe the same set of couplings via the Higgs loop contributions to the ZZZ and ZW^+W^- form factors.[17] CP-violating contributions to the triple gauge boson vertices ZZZ and ZW^+W^- vertices were first studied in Refs. [56–60]. For example, the general Lorentz structure of the $Z(P)W^+(q)W^-(\bar{q})$ vertex (with all momenta pointing into the vertex) given in Ref. [57] is

$$\Gamma_V^{\alpha\beta\mu}(q,\bar{q},P) = f_1^V(\bar{q}-q)^\mu g^{\alpha\beta} - \frac{f_2^V}{m_W^2}(\bar{q}-q)^\mu P^\alpha P^\beta + f_3^V(P^\alpha g^{\mu\beta} - P^\beta g^{\mu\alpha}) + i f_4^V(P^\alpha g^{\mu\beta} + P^\beta g^{\mu\alpha})$$
$$+ i f_5^V \epsilon^{\mu\alpha\beta\rho}(\bar{q}-q)_\rho - f_6^V \epsilon^{\mu\alpha\beta\rho} P_\rho - \frac{f_7^V}{m_W^2}(\bar{q}-q)^\mu \epsilon^{\alpha\beta\rho\sigma} P_\rho (\bar{q}-q)_\sigma. \tag{24}$$

The three form factors proportional to the Levi-Civita tensor are P violating. One can easily verify that $f_{1,2,3}^V$ separately conserve C, P, and T, whereas f_4^V is the unique form factor that is P conserving and CP violating. This form factor is generated by the bosonic sector of the extended Higgs sector provided that the scalar potential and/or vacuum is CP violating. In light of eq. (20), it follows that in the exact Higgs alignment limit, a nonzero scalar contribution to f_4 requires at least three neutral scalars beyond the SM-like Higgs boson.[18]

There are several calculations in the literature of f_4 in the complex 2HDM [56,94], in a CP-violating 3HDM with two inert doublets [31], and in a model with two Higgs doublets and a singlet [32]. Note that in the 2HDM, the contribution of the neutral scalars vanishes in the exact Higgs alignment limit. Hence, an extended Higgs sector with at least three neutral scalars beyond the SM-like Higgs boson h_1 is required to yield a nonzero value of f_4 as noted above. In practice, the maximal values for f_4 are, however, still an order of magnitude[19] away from the experimentally measured values [95,96]. Future projection for the measurement f_4 can be found in Ref. [97] for the HL-LHC and in Ref. [98] for the International Linear Collider (ILC).

The observation of a nonzero value of f_4 would provide unambiguous evidence for the existence of P-even CP violation. The main disadvantages of this observable is that it is loop suppressed and is subject to significant systematic uncertainties that must be overcome in any realistic experiment. On the other hand, f_4 is sensitive to a wider class of Higgs sectors than those that can be probed by observables examined in Sec. IV. For example, in models with two or more inert doublets, the corresponding scalar potential can contain CP-violating terms that generate neutral scalars of indefinite CP, as was shown initially in Ref. [31] and examined further in Refs. [32,41,99,100]. The P-even, CP-violating signals arising at tree level from such models cannot be probed by the methods discussed in Secs. III and IV as noted below eq. (20). Nevertheless, these inert scalars can appear in the loops that contribute to the ZZZ and ZW^+W^- form factor (since every vertex of the loop diagram involves a coupling of a pair of $\mathbb{Z}_2$-odd scalars), thereby yielding a nonzero result for f_4. Further details will be left to a future study.

VI. FINAL STATE PHOTONS AS A DIAGNOSTIC FOR *CP* VIOLATION

In our study of P-even, CP-violating phenomena at colliders, we relied on tree-level production processes at lepton colliders involving the Higgs bosons and gauge bosons. In such cases, any P-odd, CP-violating contribution to the production process arising from the Yukawa sector would be loop suppressed and hence unlikely to have a significant impact on the interpretation of the source of CP

[17] The $ZZ\gamma$ and $Z\gamma\gamma$ form factors cannot be used for this purpose, as the only scalar loop contributions involve the charged Higgs boson, which does not contribute to the P-even, CP-violating form factor.

[18] Note that there are two triangle diagrams with internal scalars that contribute at one-loop order to the ZW^+W^- form factors, consisting of an $H^+H^-h_j$ and an $h_jh_kH^+$ loop, with corresponding ZH^+H^- and Zh_jh_k vertices, respectively. Only the latter can contribute to the P-even, CP-violating form factor f_4.

[19] The contributions to f_4 in the model with two Higgs doublets and a singlet are suppressed by an order of magnitude as compared to the CP-violating 3HDM with two inert doublets, due to the presence of fewer number of inert states contributing to the ZZZ loop, along with diluted Zh_ih_j couplings (since the singlet has no direct couplings to the SM gauge bosons).

violation. In some cases, the Higgs bosons produced could decay into either two lighter Higgs bosons or into a Higgs boson and a gauge boson. In such cases, any P-odd, CP-violating contribution to the decay process arising from the Yukawa sector would again be loop suppressed. Ultimately, the Higgs bosons produced, either directly in the initial production process and/or in the decay chain of the produced Higgs boson, are identified experimentally via their fermionic decay channels. However, the presence of these fermionic channels does not obscure the original tree-level bosonic couplings involved in the original Higgs production and the bosonic Higgs decay processes. Thus, the interpretation of the P-even, CP-violating signal based on the bosonic Higgs vertices is not compromised.

If one is willing to tolerate branching ratio suppressions associated with the rarer one-loop mediated Higgs decay processes, then in principle, one could have additional channels to probe the presence of P-even CP violation in the scalar sector. In such cases, P-odd CP violation due to a fermion loop would compete at the same order with the P-even CP violation due to a bosonic loop. In this section, we explore this possibility in more detail by examining the impact of Higgs decay processes involving final state photons and Z bosons.

A. Higgs boson decays to two photons

In the absence of Yukawa couplings of the Higgs bosons, the simultaneous observations of the interactions ($i \neq j$, i, $j \neq 1$)

$$h_i \to \gamma\gamma \text{ or } Z\gamma, \quad h_j \to \gamma\gamma \text{ or } Z\gamma, \quad \text{and the } Zh_ih_j \text{ vertex} \tag{25}$$

would also constitute a signal of P-even CP violation. Once again, by taking all scalars to be P even, the existence of the Zh_ih_j vertex in a CP-conserving theory would imply that h_i and h_j have opposite C quantum numbers, whereas the observation of a $\gamma\gamma$ or $Z\gamma$ decay would imply that the corresponding neutral scalar is C even. Due to the suppressed rate for the decay of a scalar to $Z\gamma$ relative to $\gamma\gamma$, we henceforth focus only on the $\gamma\gamma$ decay mode of h_i (although the corresponding analysis for the $Z\gamma$ decay mode is similar).

.In the exact Higgs alignment limit, the $\gamma\gamma$ decay is mediated by a charged Higgs loop (since the $h_iW^+W^-$ vertex is absent for $i \neq 1$). Phenomenologically, the $h_{i,j}\gamma\gamma$ interactions may have a better discovery potential than the signals discussed in Sec. IV, despite the loop-suppression of its coupling strength. In particular, the decays $h_{i,j} \to \gamma\gamma$ are not kinematically suppressed, and the two photon signal can easily be identified experimentally as a resonance in the diphoton-invariant mass spectrum. In addition, one can probe these interactions via photon-photon scattering in a future e^+e^- linear collider or a photon collider. The observation of the three processes listed in eq. (25) requires the discovery of two new neutral Higgs bosons h_i and h_j ($i \neq j \neq 1$) in addition to the discovered SM-like Higgs boson h_1. Neither h_i nor h_j can be identified as h_1 since in the exact Higgs alignment limit the interaction Zh_ih_1 ($i \neq 1$) vanishes.

It appears that the utility of eq. (25) as a signal of CP violation is spoiled once the effects of the Yukawa couplings are included. For example, in the CP-conserving 2HDM where h_2 and h_3 are CP even and CP odd, respectively, both $h_2\gamma\gamma$ and $h_3\gamma\gamma$ couplings are generated at one loop mediated by fermions. The effective Lagrangian that governs these couplings is

$$\mathcal{L}_{\text{eff}} = g_2h_2F_{\mu\nu}F^{\mu\nu} + g_3h_3\epsilon_{\mu\nu\alpha\beta}F^{\mu\nu}F^{\alpha\beta}. \tag{26}$$

The two operators above can be experimentally distinguished. For example, the corresponding decay amplitudes have difference dependences on the photon polarizations $\boldsymbol{\varepsilon_1}$ and $\boldsymbol{\varepsilon_2}$,

$$\mathcal{A}(h_2 \to \gamma\gamma) \sim \boldsymbol{\varepsilon_1} \cdot \boldsymbol{\varepsilon_2}, \qquad \mathcal{A}(h_3 \to \gamma\gamma) \sim \boldsymbol{\varepsilon_1} \times \boldsymbol{\varepsilon_2}. \tag{27}$$

In contrast, the one-loop couplings of a scalar ϕ to $\gamma\gamma$ mediated by a charged Higgs boson can only produce an effective coupling $\phi F_{\mu\nu}F^{\mu\nu}$. Consequently, the observation of a Zh_2h_3 coupling in conjunction with evidence for the presence of the effective couplings $h_2F_{\mu\nu}F^{\mu\nu}$ and $h_3F_{\mu\nu}F^{\mu\nu}$ would constitute a signal of P-even CP violation.

B. Higgs boson decays to multivector-boson final states

Consider the implications of the simultaneous observation of the decays,

$$h_i \to \gamma\gamma, \quad \text{and} \quad h_i \to \gamma\gamma\gamma. \tag{28}$$

Since $\gamma\gamma$ is C even and $\gamma\gamma\gamma$ is C odd, it follows that, in the absence of Higgs boson couplings to fermions, the simultaneous observation the loop-induced decays exhibited in eq. (28) would be a signal for P-even CP violation. It is noteworthy that this CP-violating observable requires the discovery of only one new Higgs boson h_i (in contrast to the signals of Sec. III that rely on the Zh_ih_j coupling). However, an analysis presented in Appendix B reveals that the $h_i \to \gamma\gamma\gamma$ decay amplitude vanishes at the one-loop level (independently of the presence or absence of Higgs boson couplings to fermions). Thus, the decay rate for $h_i \to \gamma\gamma\gamma$ relative to $h_i \to \gamma\gamma$ is suppressed by both a loop factor and the three-body phase space suppression. Thus, in practice, the detection of CP violation via this scenario is not viable.

One can improve matters by replacing one or two of the photons with Z bosons. For example, consider the implications of the simultaneous observation of the decays,

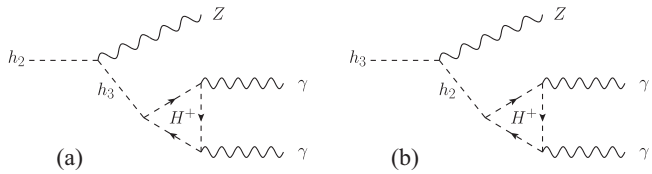

FIG. 8. Sample one-loop diagrams contributing to the decay process $h_{2,3} \to Z\gamma\gamma$.

$$h_i \to \gamma\gamma \text{ or } Z\gamma, \quad \text{and} \quad h_i \to Z\gamma\gamma. \tag{29}$$

First, suppose that the couplings of h_i to fermions are absent. In this case, we can again make use of the analysis presented in Appendix B, where one of the final state photons in Fig. 9 of Appendix B is replaced by a Z boson. We again conclude that the contributions to the one-loop matrix element for $h_i \to Z\gamma\gamma$ due to the sum of the diagrams analogous to those of Fig. 9 (as well as the corresponding diagrams where the charged Higgs loop is replaced by a charged W loop) must exactly vanish for any choice of Higgs boson state h_i. However, in contrast to $h_i \to \gamma\gamma\gamma$, additional one-loop diagrams shown in Fig. 8 contribute to $h_i \to Z\gamma\gamma$. These diagrams do not vanish. Indeed, if P and C are separately conserved, then the diagrams shown in Fig. 8(b) contribute to the C- and P-conserving decay $h_3 \to Z\gamma\gamma$ while the one-loop decay $h_3 \to \gamma\gamma/Z\gamma$ is forbidden, whereas the diagram for $h_2 \to Z\gamma\gamma$ shown in Fig. 8(a) is forbidden while the one-loop decay $h_2 \to \gamma\gamma/Z\gamma$ is allowed. These results follow in light of the absence of an $h_3H^+H^-$ vertex when CP is conserved. Thus, the simultaneous observation of the decays of eq. (29) would constitute a signal for P-even CP violation. Moreover, both decays arise at one-loop order (although, admittedly, the $Z\gamma\gamma$ final state would be suppressed relative to the $\gamma\gamma$ and $Z\gamma$ final states due to a coupling constant and the three-body phase space suppression).

If the couplings of h_i to fermions are present, then one has to reconsider the analysis in which the charged Higgs boson loop in Figs. 8(a) and 8(b) is replaced by a fermion loop. In this case, CP conservation does not forbid the simultaneous decay channels, $h_2 \to Z\gamma$ or $h_3 \to Z\gamma$. Thus, isolating any P-even, CP-violating contribution to the simultaneous observation of eq. (29) would require a separation of the CP-even and CP-odd components of the $Z\gamma$ system analogous to the discussion below eq. (26).

Finally, a similar analysis applies to

$$h_i \to \gamma\gamma \text{ or } Z\gamma, \quad \text{and} \quad h_i \to ZZ\gamma. \tag{30}$$

In particular, one simply replaces one of outgoing photons in Fig. 8 by a Z boson. Once again, this scenario is less useful than eq. (29) due to the suppression of the effective $h_iZ\gamma$ vertex relative to that of $h_i\gamma\gamma$.

VII. BEYOND THE EXACT HIGGS ALIGNMENT LIMIT

In previous sections, we focused on P-even, CP-violating signals in the bosonic sector of the 2HDM in the exact Higgs alignment limit. In this section, we shall extend our considerations to the case where there is a departure from exact Higgs alignment. The present Higgs data require that any departure from exact Higgs alignment should be small. We shall identify new P-even, CP-violating signals that, although suppressed due to approximate Higgs alignment, would provide new observables that could be probed in future experiments. Several observables for scalar sector CP violation that appear at tree level or one-loop level have been discussed in Refs. [50,52,53] and Ref. [56], respectively. In contrast to the observables introduced in Sec. III, these observables vanish in the exact Higgs alignment limit.

It is noteworthy that in the exact Higgs alignment limit, the observation of two tree-level processes is not sufficient to identify the presence of P-even CP violation. Indeed, in light of eqs. (11)–(20), it is necessary to observe at least three tree-level processes to provide evidence of P-even CP violation.[20] In contrast, if one also allows for Higgs alignment suppressed processes, then there are cases in which the observation of only two tree-level processes is enough to claim the detection of P-even CP violation. Examples of such cases are shown below.

Given that h_1 is the SM-like Higgs boson (which is a CP-even scalar), our list of interactions in eqs. (11)–(20) expands to include the following.

one Higgs alignment suppressed observables:

1. $h_iH^+H^-$, Zh_1h_i, (for $i \neq 1$), (31)

2. $h_ih_jh_j$, Zh_1h_i, (for $i, j \neq 1$), (32)

3. $h_1h_ih_j$, Zh_ih_j, (for $i, j \neq 1$ and $i \neq j$). (33)

4. $h_ih_1h_1$, $h_jH^+H^-$, Zh_ih_j, (for $i, j \neq 1$ and $i \neq j$), (34)

5. $h_kh_1h_1$, $h_ih_jh_k$, Zh_ih_j, (for $i, j, k \neq 1$ and $i \neq j$), (35)

6. $h_ih_1h_1$, $h_jh_kh_k$, Zh_ih_j, (for $i, j, k \neq 1$ and $i \neq j$); (36)

two Higgs alignment suppressed observables:

1. $h_ih_1h_1$, Zh_1h_i, (for $i \neq 1$), (37)

[20]Note that the processes exhibited in eqs. (28)–(30) are loop induced and therefore exempt from the three processes requirement.

2. $h_1 h_i h_j, \quad Z h_1 h_i, \quad h_j H^+ H^-, \quad (\text{for } i, j \neq 1 \text{ and } i \neq j),$ (38)

3. $h_i h_1 h_1, \quad h_j h_1 h_1, \quad Z h_i h_j, \quad (\text{for } i, j \neq 1 \text{ and } i \neq j),$ (39)

4. $h_1 h_i Z, \quad h_1 h_j Z, \quad Z h_i h_j, \quad (\text{for } i, j \neq 1 \text{ and } i \neq j),$ (40)

5. $h_1 h_i h_j, \quad Z h_1 h_i, \quad h_j h_k h_k, \quad (\text{for } i, j, k \neq 1 \text{ and } i \neq j);$ (41)

three Higgs alignment suppressed observables:

1. $h_i h_1 h_1, \quad h_1 h_i h_j, \quad Z h_1 h_j, \quad (\text{for } i, j \neq 1 \text{ and } i \neq j).$ (42)

The observation of any one of the combinations of observables listed in eqs. (31)–(42) would constitute a signal of P-even CP violation, under the assumption that the one-loop corrections to the above observables due to fermion loops are subdominant to the tree-level contributions (after taking into account any suppressions due to approximate Higgs alignment). If the fermion-loop contributions to the above processes are competitive with the corresponding tree-level contributions, then the distinction between P-even and P-odd CP violation becomes less clear, although the CP violation interpretation of the signal is still maintained.

If the $h_i ZZ$ vertex is included, then the presence or absence of fermion-loop contributions becomes critical to the interpretation of the signal. In the absence of fermion-loop contributions, the C and P quantum number listed in Table I can be employed to conclude that the coupling of a CP-odd scalar to ZZ would constitute evidence for CP violation. However, such a conclusion is no longer tenable if fermion-loop contributions are present, since dimension-5 operators induced by fermion loop contributions exhibited in eq. (26) demonstrate that both CP-even and CP-odd scalars can couple to ZZ in a CP-conserving theory.

For completeness, we list below additional combination of observables that can be interpreted as evidence of P-even CP violation in the absence of fermion-loop contributions:

one Higgs alignment suppressed observables:

1. $h_i ZZ, \quad h_j H^+ H^-, \quad (\text{for } i, j \neq 1 \text{ and } i \neq j) \quad (\text{only in the 2HDM}),$ (43)

2. $h_i ZZ, \quad h_j H^+ H^-, \quad Z h_i h_j, \quad (\text{for } i, j \neq 1 \text{ and } i \neq j),$ (44)

3. $h_i ZZ, \quad h_j h_k h_k, \quad Z h_i h_j, \quad (\text{for } i, j, k \neq 1 \text{ and } i \neq j),$ (45)

4. $h_k ZZ, \quad h_i h_j h_k, \quad Z h_i h_j, \quad (\text{for } i, j, k \neq 1 \text{ and } i \neq j \neq k);$ (46)

two Higgs alignment suppressed observables:

1. $h_i ZZ, \quad Z h_1 h_i, \quad (\text{for } i \neq 1),$ (47)

2. $h_i ZZ, \quad h_j h_1 h_1, \quad (\text{for } i, j \neq 1 \text{ and } i \neq j) \quad (\text{only in the 2HDM}),$ (48)

3. $h_i ZZ, \quad h_j ZZ, \quad (\text{for } i, j \neq 1 \text{ and } i \neq j) \quad (\text{only in the 2HDM}),$ (49)

4. $h_i ZZ, \quad h_j ZZ, \quad Z h_i h_j, \quad (\text{for } i, j \neq 1 \text{ and } i \neq j),$ (50)

5. $h_i ZZ, \quad h_j h_1 h_1, \quad Z h_i h_j, \quad (\text{for } i, j \neq 1 \text{ and } i \neq j);$ (51)

three Higgs alignment suppressed observables:

1. $h_i ZZ, \quad h_1 h_i h_j, \quad Z h_1 h_j, \quad (\text{for } i, j \neq 1 \text{ and } i \neq j).$ (52)

Note that the observables in eq. (40), eqs. (49)–(50), and eq. (52) appear in Refs. [50,52,53] where decay processes are studied.

In principle, one could replace ZZ with $\gamma\gamma$ (or $Z\gamma$) in eqs. (43)–(52). If fermion loops are absent, then the observation of any of the corresponding ten sets of observables could be interpreted as evidence of P-even CP violation. The $h_i \gamma\gamma$ one-loop amplitude in each case would be mediated by a W or charged Higgs boson loop. For $i \neq 1$, the W-loop contribution would be Higgs

alignment suppressed, whereas the charged Higgs loop contribution would be present in the exact Higgs alignment limit. However, if $h_i \to ZZ$ is kinematically allowed, then the tree-level decay would dominate the corresponding $h_i \to \gamma\gamma$ decay, in which case the observables listed in eqs. (43)–(52) would be the preferred signatures of P-even CP violation. If fermion loops are present, then the fermion loop contribution to the $h_i\gamma\gamma$ decay amplitude is not Higgs alignment suppressed. On the other hand, as discussed in Sec. VI A, the observation of the $\gamma\gamma$ decay mode would not constitute evidence for CP violation unless the photon polarizations are measured to distinguish the operators exhibited in eq. (27).

As noted above, if the h_i ($i \neq 1$) couple to fermions, then the presence or absence of the h_iZZ coupling by itself sheds no light on the existence of CP violation in the scalar sector in the exact Higgs alignment limit. Since the h_iZZ tree-level coupling for $i \neq 1$ is absent in the exact Higgs alignment limit, this coupling is only generated at the loop level via fermion loop contributions. Indeed, as shown in Ref. [101] for the CP-conserving 2HDM where h is identified as the observed Higgs boson of mass 125 GeV, the decay width of $A \to ZZ$ is of the same order of magnitude as $H \to ZZ$ in the exact Higgs alignment limit. Therefore, when the h_iZZ couplings ($i \neq 1$) are of the same order, one can no longer use them to probe CP violation. Away from the exact Higgs alignment limit, tree-level h_iZZ couplings (for $i \neq 1$) may be present. If the size of these tree-level couplings is parametrically larger than the corresponding one-loop amplitude generated by fermion loop contributions, then the presence of P-even CP violation can be probed using the observables listed in eqs. (43)–(52) in the approximation that the one-loop contributions can be neglected. In practice, determining the conditions where the latter approximation is valid is model dependent. For example, in models with additional particles beyond the scalar sector that carry electroweak quantum numbers (e.g., vectorlike quarks or supersymmetric particles), additional contributions to the one-loop amplitude will make it more difficult to distinguish between tree-level effects suppressed in the approximate Higgs alignment limit and loop-level effects.

In the scenarios presented in Sec. IV D, we focused on observables that depended on tree-level couplings that were not suppressed in the Higgs alignment limit. Given that the results exhibited in this section were obtained in the exact Higgs alignment limit, one can ask whether the potential signals of P-even CP violation are robust as one moves away from exact Higgs alignment. For example, away from the Higgs alignment limit, the triple scalar couplings are modified; in particular, they depend on additional parameters of the scalar potential.[21] Hence, both the production cross section and branching ratios obtained in Sec. IV D will be modified. The modifications are to some extent random because the processes of interest are now controlled by different couplings. Nevertheless, by combining all possible sets of CP-violating observables, the chances of being able to probe P-even CP violation in extended Higgs sectors are very good if the scalars h_i ($i \neq 1$) are not too heavy.

[21]In contrast, in the exact Higgs alignment limit, each $h_iH^+H^-$ coupling is proportional to Λ_i [cf. eq. (23)].

VIII. CONCLUSIONS

There is vast literature (e.g., see Refs. [37–46]) discussing CP-violating observables that derive from the P-violating, C-conserving neutral Higgs-fermion Yukawa couplings in models with an extended Higgs sector beyond the Standard Model. However, additional sources of CP violation of a different nature can arise from the pure bosonic sector of the model. Indeed, in a theory consisting only of bosonic fields (scalars and gauge bosons), CP-violating phenomena, if present, must be associated with C-violating observables. This statement is independent of the number and representation of the multiplets of scalar fields and the choice of gauge group. Hence, if nature employs an extended Higgs sector, then one needs to identify physical observables that either receive negligible fermionic contributions or are completely insensitive to the presence of the fermions in order to experimentally verify the presence of P-even, CP-violating processes.

A combination of three bosonic decays in the 2HDM that signal the presence of P-even CP violation was proposed in Refs. [50,52,53] and involves the interaction of the Z boson with a pair of neutral scalars, Zh_ih_j ($1 \leq i < j \leq 3$). If CP is conserved, then h_i and h_j must have opposite sign CP quantum numbers. Thus, the observation of all three interactions (e.g., via the three decays $h_3 \to h_2Z$, $h_3 \to h_1Z$, and $h_2 \to h_1Z$) necessarily implies that CP must be violated. However, after identifying h_1 with the Higgs boson observed at the LHC, the decay rates for two of the three processes cited above vanish in the exact Higgs alignment limit (where the tree-level properties of h_1 coincide with those of the SM Higgs boson). Since the LHC Higgs data show a clear preference for a SM-like Higgs boson, it follows that the CP-violating signal considered above is highly suppressed.

In this work, we have found and listed all possible combinations of bosonic interactions that can be employed to identify the presence of P-even, CP-violating phenomena that are not suppressed in the Higgs alignment limit. Most of these combinations rely on the discovery of three new scalars (one of which is charged), except for one case where only two new neutral scalars are needed. For example, the simultaneous observation of the vertices Zh_2h_3, $h_2H^+H^-$, and $h_3H^+H^-$ would provide unambiguous evidence for P-even CP violation. Moreover, the interactions that we have identified can be quite large and give rise to detectable signals at future multi-TeV

colliders. For completeness, we have also listed all possible combinations that include interactions with suppressed couplings in the Higgs alignment limit, classifying them by the number of suppressed interactions.

Uncovering evidence for P-even CP violation depends on the detection of new heavy scalar particles. At the LHC, the decays of the new scalars provide an opportunity to probe P-even, CP-violating processes if a sufficient number of appropriate final states are accessible. When considering the combination of Higgs decays, kinematic constraints due to the scalar masses can preclude probing a specific vertex. A more robust exploration of P-even, CP-violating phenomena can be carried out in an experimentally clean environment such as a lepton collider, assuming that the production of the heavy scalars is kinematically accessible. At lepton colliders, the observation of P-even, CP-violating processes can make use of a combination of production and decay mechanisms that do not involve the Higgs-fermion Yukawa couplings at leading order.

In Sec. IV, we performed a phenomenological study for various future multi-TeV lepton colliders. We demonstrated that, given the CM energies and total integrated luminosities of CLIC and of a planned muon collider, many combinations of production processes and/or decay channels are within the reach of these machines. The simplest production process is $\ell^+\ell^- \to h_2 h_3$ via s-channel Z exchange, where ℓ can be either an electron or a muon. If kinematically allowed, both h_2 and h_3 could decay to a pair of charged Higgs bosons, H^+H^-. Alternatively, one can combine the former production process with $\ell^+\ell^- \to h_2 h_2 h_3$ and $\ell^+\ell^- \to h_2 h_3 h_3$. Using only production processes has the clear advantage of being dependent only on the collider CM energy. As these are s-channel processes, colliders with lower CM energy are better suited to probe them. However, the production cross sections for very heavy scalars are rather small, especially in the case of a three particle final state.

There are also t-channel $\gamma\gamma$ processes, such as $\ell^+\ell^- \to \ell^+\ell^- H^+H^- h_i$, whose cross sections grow logarithmically with the collider CM energy and are best suited for higher energy colliders. These t-channel cross sections yield viable signals at a muon collider with a CM energy of order 10 TeV. However, the best option to probe processes such as $\gamma\gamma \to h_i H^+H^-$ is to make use of a (hypothetical) photon collider option at CLIC. We concluded the phenomenological study of Sec. IV with a brief description of the possible final states. In order to find the exact reach of each collider, one needs to establish a set of realistic benchmarks by considering a full experimental analysis by taking into account the complete set of backgrounds to the final state under consideration together with the detector effects. This task is left to a future study.

This paper has focused primarily on P-even, CP-violating phenomena associated with tree-level processes. Nevertheless, there are some cases in which loop-induced processes can play an important role. A measurement of a P-even, CP-violating form factor in the loop-induced ZZZ and ZW^+W^- vertex provides a promising approach for detecting P-even, CP-violating phenomena. In principle, such phenomena could also be probed by loop-induced decays of scalars into final state photons and Z bosons. For example, the observation of $h_k \to \gamma\gamma$ (γZ) together with $h_k \to \gamma\gamma\gamma$ ($\gamma\gamma Z$ or γZZ) would constitute a signal of P-even CP violation if the purely bosonic loop contributions can be isolated. However, we have shown that the amplitude for the $\gamma\gamma\gamma$ decay mode vanishes exactly at one-loop order (whereas the corresponding one-loop amplitudes for the $\gamma\gamma Z$ and γZZ final states are nonzero). Moreover, due to extra coupling constant and phase space suppression factors that arise in computing the decay rates for the three-body final states, we concluded that the detection of P-even CP violation via the multiphoton/Z decay channels is completely impractical.

The LHC has just begun to probe the existence of C-even, CP-violating interactions of the Higgs boson in the top-quark and tau-lepton Yukawa couplings (which requires the observation of both scalar and pseudoscalar couplings of the neutral Higgs boson to a fermion-antifermion pair). The observation of such interactions would be strongly suggestive of an extended Higgs sector in which the SM-like Higgs boson is not quite an eigenstate of CP due to the mixing with additional scalar degrees of freedom. In such a framework, one would also expect the existence of P-even, CP-violating interactions. However, such interactions arise solely from the bosonic sector of the theory and as such cannot be associated with an experimental observable that involves a single scalar state. Thus, the observation of P-even CP violation is far more challenging and is possible at future runs of the LHC only in very special circumstances. Ultimately, to achieve a more robust probe of P-even, CP-violating phenomena, the relatively clean environment of a future multi-TeV lepton collider will be required, where the cross sections for multiple heavy scalar production are large enough to yield a viable experimental signal. Indeed, the detection of the presence or absence of a P-even, CP-violating signal would provide crucial information concerning the fundamental nature of the scalar sector.

ACKNOWLEDGMENTS

H. E. H. and V. K. are grateful for many valuable conversations with Tim Stefaniak and Scott Thomas, who collaborated with us on the initial phase of this project. R. S. thanks Richard Ruiz and Jonas Wittbrodt for discussions. We also acknowledge discussions with Michael Peskin concerning futuristic very high energy $\gamma\gamma$ colliders. H. E. H. is supported in part by the U.S. Department of Energy Grant No. DE-SC0010107. V. K. acknowledges financial support from the Academy of Finland projects

"Particle cosmology and gravitational waves," Grant No. 320123; "Particle cosmology beyond the Standard Model," Grant No. 310130; and the Science Foundation Ireland Grant No. 21/PATH-S/9475 (MOREHIGGS) under the SFI-IRC Pathway Programme. Both H. E. H. and V. K. acknowledge the support of H2020-MSCA-RISE-2014 Grant No. 645722 (NonMinimalHiggs), which provided funds for two separate month-long visits by V. K. to the Santa Cruz Institute for Particle Physics (SCIPP) and for the travel of H. E. H. to the 2019 NonMinimalHiggs conference at the University of Helsinki. Both visits were highly productive in advancing this work, and H. E. H. and V. K. are grateful for the hospitality furnished by SCIPP and the University of Helsinki. R. S. is supported by FCT under Contracts No. UIDB/00618/2020, No. UIDP/00618/2020, No. PTDC/FIS-PAR/31000/2017, No. CERN/FIS-PAR/0002/2017, and No. CERN/FIS-PAR/0014/2019. H. E. H., V. K., and R. S. also benefited from discussions that took place at the University of Warsaw during visits supported by the HARMONIA project of the National Science Centre, Poland, under Contract No. UMO-2015/18/M/ST2/00518 (2016–2021).

APPENDIX A: THEORETICAL ASPECTS OF THE 2HDM

In this Appendix, we briefly introduce the 2HDM and identify a convenient set of parameters that will provide the basis for the parameter choices employed in this work. We survey the various couplings of the Higgs scalars (to gauge bosons, Higgs bosons, and fermions) and discuss the Higgs alignment limit, in which the tree-level properties of one of the neutral scalars coincides with those of the Standard Model Higgs boson.

The fields of the 2HDM consist of two identical complex hypercharge-1, SU (2) doublet scalar fields $\Phi_a(x) \equiv (\Phi_a^+(x), \Phi_a^0(x))$, where the "Higgs flavor" index $a = 1$, 2 labels the two Higgs doublet fields. The most general renormalizable $\mathrm{SU}(2)_L \times \mathrm{U}(1)_Y$-invariant scalar potential is given in the Φ-basis by

$$\mathcal{V} = m_{11}^2 \Phi_1^\dagger \Phi_1 + m_{22}^2 \Phi_2^\dagger \Phi_2 - [m_{12}^2 \Phi_1^\dagger \Phi_2 + \mathrm{H.c.}] + \frac{1}{2}\lambda_1 (\Phi_1^\dagger \Phi_1)^2 + \frac{1}{2}\lambda_2 (\Phi_2^\dagger \Phi_2)^2 + \lambda_3 (\Phi_1^\dagger \Phi_1)(\Phi_2^\dagger \Phi_2) + \lambda_4 (\Phi_1^\dagger \Phi_2)(\Phi_2^\dagger \Phi_1) + \left\{ \frac{1}{2}\lambda_5 (\Phi_1^\dagger \Phi_2)^2 + [\lambda_6 (\Phi_1^\dagger \Phi_1) + \lambda_7 (\Phi_2^\dagger \Phi_2)] \Phi_1^\dagger \Phi_2 + \mathrm{H.c.} \right\}, \tag{A1}$$

where m_{11}^2, m_{22}^2, and $\lambda_1, \ldots, \lambda_4$ are real parameters and m_{12}^2, λ_5, λ_6, and λ_7 are potentially complex parameters. We assume that the parameters of the scalar potential are chosen such that the minimum of the scalar potential respects the $\mathrm{U}(1)_{\mathrm{EM}}$ gauge symmetry.[22] Then, the scalar field vevs are of the form

$$\langle \Phi_a \rangle = \frac{v}{\sqrt{2}} \begin{pmatrix} 0 \\ \hat{v}_a \end{pmatrix}, \tag{A2}$$

where $\hat{v}$ is a complex vector of unit norm,

$$\hat{v} = (\hat{v}_1, \hat{v}_2) = (c_\beta, s_\beta e^{i\xi}), \tag{A3}$$

and $c_\beta \equiv \cos\beta$ and $s_\beta \equiv \sin\beta$, $0 \le \beta \le \frac{1}{2}\pi$, $0 \le \xi < 2\pi$, and v is determined by the Fermi constant,

$$v \equiv \frac{2m_W}{g} = (\sqrt{2} G_F)^{-1/2} \simeq 246 \text{ GeV}. \tag{A4}$$

[22]As shown in Refs. [102,103], given a generic 2HDM tree-level scalar potential that has a minimum which respects $\mathrm{U}(1)_{\mathrm{EM}}$, then any competing stationary point that breaks the $\mathrm{U}(1)_{\mathrm{EM}}$ symmetry is a saddle point that lies above the symmetry conserving vacuum.

1. Higgs basis

It is convenient to introduce the Higgs basis as follows. Starting from a generic Φ-basis, the Higgs basis fields $\mathcal{H}_1$ and $\mathcal{H}_2$ are defined by the linear combinations of Φ_1 and Φ_2 such that $\langle \mathcal{H}_1^0 \rangle = v/\sqrt{2}$ and $\langle \mathcal{H}_2^0 \rangle = 0$. That is,

$$\mathcal{H}_1 \equiv c_\beta \Phi_1 + s_\beta e^{-i\xi} \Phi_2, \qquad \mathcal{H}_2 = e^{i\eta}[-s_\beta e^{i\xi} \Phi_1 + c_\beta \Phi_2], \tag{A5}$$

where we have introduced (following Ref. [104]) the complex phase factor $e^{i\eta}$ to account for the nonuniqueness of the Higgs basis, since one is always free to rephase the Higgs basis field whose vacuum expectation value vanishes. In particular, $e^{i\eta}$ is a pseudoinvariant quantity that is rephased under the unitary basis transformation, $\Phi_a \to U_{a\bar{b}} \Phi_b$, as[23]

$$e^{i\eta} \to (\det U)^{-1} e^{i\eta}, \tag{A6}$$

where $\det U$ is a complex number of unit modulus. Equivalently, one can write

[23]The use of unbarred and barred indices follows the conventions introduced in Ref. [15].

$$\mathcal{H}_1 = (\mathcal{H}_1^+, \mathcal{H}_1^0) \equiv \hat{v}_{\bar{a}}^* \Phi_a, \quad \mathcal{H}_2 = (\mathcal{H}_2^+, \mathcal{H}_2^0) \equiv e^{i\eta} \hat{w}_{\bar{a}}^* \Phi_a, \tag{A7}$$

where there is an implicit sum over unbarred/barred index pairs and

$$\hat{w}_b = \hat{v}_{\bar{a}}^* \epsilon_{ab} \quad (\epsilon_{12} = -\epsilon_{21} = 1 \text{ and } \epsilon_{11} = \epsilon_{22} = 0) \tag{A8}$$

is a unit vector that is orthogonal to $\hat{v}$ (i.e., $\hat{v}_{\bar{b}}^* \hat{w}_b = 0$). Under a U(2) basis transformation,

$$\hat{v}_a \to U_{a\bar{b}} \hat{v}_b, \quad \text{which implies that} \quad \hat{w}_a \to (\det U)^{-1} U_{a\bar{b}} \hat{w}_b. \tag{A9}$$

In light of eqs. (A6)–(A9), it follows that both $\mathcal{H}_1$ and $\mathcal{H}_2$ are invariant fields with respect to U(2) basis transformations.

In terms of the Higgs basis fields defined in eq. (A5), the scalar potential is given by

$$\begin{aligned}\mathcal{V} = {} & Y_1 \mathcal{H}_1^\dagger \mathcal{H}_1 + Y_2 \mathcal{H}_2^\dagger \mathcal{H}_2 + [Y_3 e^{-i\eta} \mathcal{H}_1^\dagger \mathcal{H}_2 + \text{H.c.}] + \frac{1}{2} Z_1 (\mathcal{H}_1^\dagger \mathcal{H}_1)^2 + \frac{1}{2} Z_2 (\mathcal{H}_2^\dagger \mathcal{H}_2)^2 \\ & + Z_3 (\mathcal{H}_1^\dagger \mathcal{H}_1)(\mathcal{H}_2^\dagger \mathcal{H}_2) + Z_4 (\mathcal{H}_1^\dagger \mathcal{H}_2)(\mathcal{H}_2^\dagger \mathcal{H}_1) + \left\{ \frac{1}{2} Z_5 e^{-2i\eta} (\mathcal{H}_1^\dagger \mathcal{H}_2)^2 + [Z_6 e^{-i\eta} (\mathcal{H}_1^\dagger \mathcal{H}_1) + Z_7 e^{-i\eta} (\mathcal{H}_2^\dagger \mathcal{H}_2)] \mathcal{H}_1^\dagger \mathcal{H}_2 + \text{H.c.} \right\}.\end{aligned} \tag{A10}$$

The coefficients of the quadratic and quartic terms of the scalar potential in eq. (A10) are independent of the initial choice of the Φ-basis. It then follows that Y_3, Z_5, Z_6, and Z_7 are also pseudoinvariant quantities that are rephased under $\Phi_a \to U_{a\bar{b}} \Phi_b$ as follows:

$$\begin{aligned}&[Y_3, Z_6, Z_7] \to (\det U)^{-1} [Y_3, Z_6, Z_7] \quad \text{and} \\ &\qquad Z_5 \to (\det U)^{-2} Z_5.\end{aligned} \tag{A11}$$

The minimization of the scalar potential in the Higgs basis yields

$$Y_1 = -\frac{1}{2} Z_1 v^2, \qquad Y_3 = -\frac{1}{2} Z_6 v^2. \tag{A12}$$

2. Physical mass eigenstates

Given the scalar potential and its minimization conditions, one can determine the masses of the neutral scalars. After removing the massless Goldstone boson, $G^0 = \sqrt{2}\text{Im}\mathcal{H}_1^0$, from the 4×4 neutral scalar squared-mass matrix, the physical neutral scalar mass-eigenstate fields are obtained by diagonalizing the resulting 3×3 neutral scalar squared-mass matrix,

$$\mathcal{M}^2 = v^2 \begin{pmatrix} Z_1 & \text{Re}(Z_6 e^{-i\eta}) & -\text{Im}(Z_6 e^{-i\eta}) \\ \text{Re}(Z_6 e^{-i\eta}) & \frac{1}{2}[Z_{34} + \text{Re}(Z_5 e^{-2i\eta})] + Y_2/v^2 & -\frac{1}{2}\text{Im}(Z_5 e^{-2i\eta}) \\ -\text{Im}(Z_6 e^{-i\eta}) & -\frac{1}{2}\text{Im}(Z_5 e^{-2i\eta}) & \frac{1}{2}[Z_{34} - \text{Re}(Z_5 e^{-2i\eta})] + Y_2/v^2 \end{pmatrix}, \tag{A13}$$

with respect to the $\{\sqrt{2}\text{Re}\mathcal{H}_1^0 - v, \sqrt{2}\text{Re}\mathcal{H}_2^0, \sqrt{2}\text{Im}\mathcal{H}_2^0\}$ basis, where $Z_{34} \equiv Z_3 + Z_4$. The squared masses of the physical neutral scalars, denoted by m_k^2 ($k = 1, 2, 3$) with no implied mass ordering, are the eigenvalues of $\mathcal{M}^2$, which are independent of the choice of η.

The real symmetric squared-mass matrix $\mathcal{M}^2$ can be diagonalized by a real orthogonal transformation of unit determinant,

$$R\mathcal{M}^2 R^\mathsf{T} = \text{diag}(m_1^2, m_2^2, m_3^2), \tag{A14}$$

where $R \equiv R_{12} R_{13} R_{23}$ is the product of three rotation matrices parametrized by θ_{12}, θ_{13}, and θ_{23}, respectively [105]. Since the matrix elements of $\mathcal{M}^2$ are independent of the scalar field basis, it follows that the mixing angles θ_{ij} are invariant parameters. The physical neutral mass-eigenstate scalar fields are

$$h_k = q_{k1}(\sqrt{2}\text{Re}\mathcal{H}_1^0 - v) + \frac{1}{\sqrt{2}}(q_{k2}^* \mathcal{H}_2^0 e^{i\theta_{23}} + \text{H.c.}), \tag{A15}$$

where q_{k1} and q_{k2} are exhibited in Table IV. The charged scalar mass eigenstates are defined by

$$G^\pm = \mathcal{H}_1^\pm, \qquad H^\pm \equiv e^{\pm i\theta_{23}} \mathcal{H}_2^\pm, \tag{A16}$$

where we have rephased the charged Higgs fields as a matter of convenience. The mass of the charged Higgs scalar is given by

TABLE IV. The U(2)-invariant quantities $q_{k\ell}$ are functions of the neutral Higgs mixing angles θ_{12} and θ_{13}, where $c_{ij} \equiv \cos\theta_{ij}$ and $s_{ij} \equiv \sin\theta_{ij}$. The angles θ_{12} and θ_{23} are defined modulo π. By convention, we take $0 \leq c_{12},\, c_{13} \leq 1$.

k	q_{k1}	q_{k2}
1	$c_{12}c_{13}$	$-s_{12} - ic_{12}s_{13}$
2	$s_{12}c_{13}$	$c_{12} - is_{12}s_{13}$
3	s_{13}	ic_{13}

$$m_{H^\pm}^2 = Y_2 + \frac{1}{2}Z_3 v^2. \tag{A17}$$

Inverting eq. (A15), one can now express the Higgs basis fields in terms of the mass eigenstate fields,

$$\mathcal{H}_1 = \begin{pmatrix} G^+ \\ \frac{1}{\sqrt{2}}\left(v + iG + \sum_{k=1}^3 q_{k1}h_k\right) \end{pmatrix},$$
$$e^{i\theta_{23}}\mathcal{H}_2 = \begin{pmatrix} H^+ \\ \frac{1}{\sqrt{2}}\sum_{k=1}^3 q_{k2}h_k \end{pmatrix}. \tag{A18}$$

In light of eq. (A18), the parameter θ_{23} can be eliminated by rephasing $\mathcal{H}_2 \to e^{-i\theta_{23}}\mathcal{H}_2$. Thus, without loss of generality, we shall henceforth set $\theta_{23} = 0$.

If we denote the physical neutral scalar masses by m_k ($k = 1, 2, 3$), then the equation for the diagonalization of the neutral scalar squared-mass matrix yields the following squared mass sum rules (e.g., see eqs. (47)–(50) of Ref. [104]):

$$Z_1 = \frac{1}{v^2}\sum_{k=1}^3 m_k^2 q_{k1}^2, \tag{A19}$$

$$Z_4 = \frac{1}{v^2}\left[\sum_{k=1}^3 m_k^2|q_{k2}|^2 - 2m_{H^\pm}^2\right], \tag{A20}$$

$$Z_5 e^{-2i\eta} = \frac{1}{v^2}\sum_{k=1}^3 m_k^2 (q_{k2}^*)^2, \tag{A21}$$

$$Z_6 e^{-i\eta} = \frac{1}{v^2}\sum_{k=1}^3 m_k^2 q_{k1} q_{k2}^*. \tag{A22}$$

Due to eqs. (A6) and (A11), the quantities $Z_5 e^{-2i\eta}$ and $Z_6 e^{-i\eta}$ are basis-invariant quantities.

More explicitly, eqs. (A19)–(A22) yield the following expressions:

$$Z_1 v^2 = m_1^2 c_{12}^2 c_{13}^2 + m_2^2 s_{12}^2 c_{13}^2 + m_3^2 s_{13}^2, \tag{A23}$$

$$Z_4 v^2 = m_1^2 + m_2^2 - c_{13}^2(c_{12}^2 m_1^2 + s_{12}^2 m_2^2 - m_3^2) - 2m_{H^\pm}^2, \tag{A24}$$

$$\mathrm{Re}(Z_6 e^{-i\eta})v^2 = c_{13}s_{12}c_{12}(m_2^2 - m_1^2), \tag{A25}$$

$$\mathrm{Im}(Z_6 e^{-i\eta})v^2 = s_{13}c_{13}(c_{12}^2 m_1^2 + s_{12}^2 m_2^2 - m_3^2), \tag{A26}$$

$$\mathrm{Re}(Z_5 e^{-2i\eta})v^2 = (c_{12}^2 - s_{12}^2)(m_2^2 - m_1^2) + c_{13}^2(c_{12}^2 m_1^2 + s_{12}^2 m_2^2 - m_3^2), \tag{A27}$$

$$\mathrm{Im}(Z_5 e^{-2i\eta})v^2 = 2s_{12}c_{12}s_{13}(m_2^2 - m_1^2). \tag{A28}$$

Finally, one additional relation of significance is the trace condition,

$$\mathrm{Tr}\mathcal{M}^2 = \sum_{k=1}^3 m_k^2 = 2Y^2 + (Z_1 + Z_{34})v^2 = 2m_{H^\pm}^2 + (Z_1 + Z_4)v^2. \tag{A29}$$

3. Parameter set of the bosonic sector of the 2HDM

Let us now count the parameters that govern the most general 2HDM. In light of eq. (A12), it follows that the 2HDM is governed by six real parameters, v, Y_2, Z_1, Z_2, Z_3, and Z_4 and three complex parameters Z_5, Z_6, and Z_7 for a total of 12 real parameters, where $v = 246$ GeV. However, due to the presence of η in eq. (A10), we are free to rephase the Higgs basis fields. In particular, consider what happens if one transforms between two Higgs bases. That is, suppose that $\langle\Phi_1^0\rangle = v/\sqrt{2}$ and $\langle\Phi_2^0\rangle = 0$. To transform to another Higgs basis, one can employ the U(2) transformation $\Phi_a \to U_{a\bar{b}}\Phi_b$, where $U = \mathrm{diag}(1, e^{i\chi})$. Then, eq. (A6) implies that $\eta \to \eta - \chi$. It then follows that

$$[Y_3, Z_6, Z_7] \to e^{-i\chi}[Y_3, Z_6, Z_7] \quad \text{and} \quad Z_5 \to e^{-2i\chi}Z_5. \tag{A30}$$

In contrast, Y_1, Y_2, and $Z_{1,2,3,4}$ are invariant when transforming between two Higgs bases. This means that among the three complex parameters, Z_5, Z_6, and Z_7, there are only five independent real physical degrees of freedom. Thus, in total there are 11 real parameters that govern the most general 2HDM.

However, it is more convenient to choose a different set of parameters to define the most general 2HDM. Here is the list:

$$v,\quad m_1,\quad m_2,\quad m_3,\quad m_{H^\pm},\quad \theta_{12},\quad \theta_{13},\quad Z_2,\quad Z_3,\quad Z_7 e^{-i\eta}. \tag{A31}$$

This list includes nine real parameters and one complex parameter $Z_7 e^{-i\eta}$ for a total of 11 real parameters that fix the 2HDM model. Note that all parameters on this list are basis-invariant quantities. In particular, one cannot

"rephase" the complex parameter $Z_7 e^{-i\eta}$ to remove one degree of freedom.

It is often assumed that the scalar potential exhibits a $\mathbb{Z}_2$ symmetry, where Φ_1 is unchanged and $\Phi_2 \to -\Phi_2$ in some scalar field basis. We will allow this symmetry to be softly broken by the dimension-2 squared-mass terms of the scalar potential, in which case there exists a Φ-basis where $\lambda_6 = \lambda_7 = 0$ in the notation of eq. (A1). Such a basis will be called the $\mathbb{Z}_2$ basis. As shown in Ref. [104], a $\mathbb{Z}_2$-basis exists if and only if the following relation is satisfied,

$$(Z_1 - Z_2)[Z_{34}Z_{67}^* - Z_1 Z_7^* - Z_2 Z_6^* + Z_5^* Z_{67}] - 2Z_{67}^*(|Z_6|^2 - |Z_7|^2) = 0, \tag{A32}$$

where $Z_{34} \equiv Z_3 + Z_4$ and $Z_{67} \equiv Z_6 + Z_7$. Since eq. (A32) is linear in Z_3, we will use this equation to solve for Z_3 and remove it from the list given in eq. (A31). In the special case of $Z_1 = Z_2$, $Z_5 \neq 0$ and $Z_{67} \neq 0$, eq. (A32) must be replaced by the two conditions,

$$\mathrm{Im}(Z_5^* Z_{67}^2) = 0, \qquad |Z_6| = |Z_7|, \qquad \text{if } Z_1 = Z_2, \qquad Z_5 \neq 0 \quad \text{and} \quad Z_{67} \neq 0. \tag{A33}$$

We can specify the $\mathbb{Z}_2$ basis by providing expressions for β and ξ [which are defined in eq. (A3)]. Assuming that $Z_{67} \neq 0$,

$$s_{2\beta} = \frac{2|Z_{67}|}{\sqrt{(Z_2 - Z_1)^2 + 4|Z_{67}|^2}}, \qquad c_{2\beta} = \frac{\pm(Z_2 - Z_1)}{\sqrt{(Z_2 - Z_1)^2 + 4|Z_{67}|^2}}, \tag{A34}$$

where by convention, $0 \leq \beta \leq \frac{1}{2}\pi$. In particular,

$$\tan\beta = \sqrt{\frac{1 - c_{2\beta}}{1 + c_{2\beta}}}, \qquad e^{i(\xi+\eta)} = \left(\frac{Z_2 - Z_1}{2Z_{67}e^{-i\eta}}\right)\frac{s_{2\beta}}{c_{2\beta}}. \tag{A35}$$

The twofold ambiguity in the choice of the sign of $c_{2\beta}$ corresponds to the fact that the conditions, $\lambda_6 = \lambda_7 = 0$, are preserved under the interchange $\Phi_1 \leftrightarrow \Phi_2$.

Given the list of parameters of eq. (A31), we can use θ_{12} and θ_{13} to determine the $q_{k\ell}$ in Table IV. Then, we can determine the real parameters Z_1 and Z_4 and the complex parameters $Z_5 e^{-2i\eta}$ and $Z_6 e^{-i\eta}$ using eqs. (A19)–(A22). Finally, Y_2 is fixed by eq. (A17).

4. 2HDM bosonic interactions

The couplings of Goldstone bosons and Higgs bosons to gauge bosons depend only on the q_{kj} and the electroweak $\mathrm{SU}(2)_L$ and $\mathrm{U}(1)_Y$ gauge coupling parameters g and g' as

$$\mathcal{L}_{VVH} = \left(g m_W W_\mu^+ W^{\mu-} + \frac{g}{2c_W} m_Z Z_\mu Z^\mu\right) q_{k1} h_k + e m_W A^\mu (W_\mu^+ G^- + W_\mu^- G^+) - g m_Z s_W^2 Z^\mu (W_\mu^+ G^- + W_\mu^- G^+), \tag{A36}$$

$$\begin{aligned}\mathcal{L}_{VVHH} = {} & \left[\frac{1}{4} g^2 W_\mu^+ W^{\mu-} + \frac{g^2}{8c_W^2} Z_\mu Z^\mu\right](G^0 G^0 + h_k h_k) \\ & + \left[\frac{1}{2} g^2 W_\mu^+ W^{\mu-} + e^2 A_\mu A^\mu + \frac{g^2}{c_W^2}\left(\frac{1}{2} - s_W^2\right)^2 Z_\mu Z^\mu + \frac{2ge}{c_W}\left(\frac{1}{2} - s_W^2\right) A_\mu Z^\mu\right](H^+ H^- + G^+ G^-) \\ & + \left\{\left(\frac{1}{2} e g A^\mu W_\mu^+ - \frac{g^2 s_W^2}{2c_W} Z^\mu W_\mu^+\right)(q_{k1} G^- + q_{k2} H^-) h_k + \text{H.c.}\right\} \\ & + \left\{\frac{1}{2} i e g A^\mu W_\mu^+ G^- G^0 - \frac{i g^2 s_W^2}{2c_W} Z^\mu W_\mu^+ G^- G^0 + \text{H.c.}\right\},\end{aligned} \tag{A37}$$

$$\begin{aligned}\mathcal{L}_{VHH} = {} & -\frac{g}{4c_W}\epsilon_{jk\ell} q_{\ell 1} Z^\mu h_j \overleftrightarrow{\partial}_\mu h_k - \frac{1}{2} g\{i W_\mu^+ [q_{k1} G^- \overleftrightarrow{\partial}^\mu h_k + q_{k2} H^- \overleftrightarrow{\partial}^\mu h_k] + \text{H.c.}\} + \frac{g}{2c_W} q_{k1} Z^\mu G^0 \overleftrightarrow{\partial}_\mu h_k \\ & + \frac{1}{2} g(W_\mu^+ G^- \overleftrightarrow{\partial}^\mu G^0 + W_\mu^- G^+ \overleftrightarrow{\partial}^\mu G^0) + \left[i e A^\mu + \frac{i g}{c_W}\left(\frac{1}{2} - s_W^2\right) Z^\mu\right](G^+ \overleftrightarrow{\partial}_\mu G^- + H^+ \overleftrightarrow{\partial}_\mu H^-),\end{aligned} \tag{A38}$$

where $s_W \equiv \sin\theta_W$, $c_W \equiv \cos\theta_W$, and the sum over pairs of repeated indices j, $k = 1, 2, 3$ is implied.

The cubic and quartic scalar self-couplings can be expressed in terms of v, the q_{kj}, $Z_1, \ldots Z_4$, $Z_5 e^{-2i\eta}$, $Z_6 e^{-i\eta}$, and $Z_7 e^{-i\eta}$ as shown in Ref. [105]. For convenience of the presentation, we introduce the following notation:

$$\bar{Z}_5 \equiv Z_5 e^{-2i\eta}, \qquad \bar{Z}_6 \equiv Z_6 e^{-i\eta}, \qquad \bar{Z}_7 \equiv Z_7 e^{-i\eta}. \tag{A39}$$

The complete list of cubic scalar couplings is exhibited in Table V.

TABLE V. Nonvanishing cubic scalar self-couplings of the most general 2HDM. The indices j, k, and ℓ are distinct integers $\in \{1,2,3\}$. To obtain the corresponding Feynman rules, multiply the self-couplings listed above by $-i$. Charged fields point *into* the vertex. The cubic self-couplings not listed above, such as GGG, Gh_jh_j, GG^+G^-, GH^+H^-, and $GG^\pm H^\mp$, vanish exactly.

Vertex	Self-coupling
Gh_jh_k	$v[\mathrm{Im}(q_{j2}q_{k2}\bar{Z}_5)+q_{j1}\mathrm{Im}(q_{k2}\bar{Z}_6)+q_{k1}\mathrm{Im}(q_{j2}\bar{Z}_6)]=\epsilon_{jk\ell}(m_j^2-m_k^2)q_{\ell 1}/v$
GGh_j	$v[q_{j1}Z_1+\mathrm{Re}(q_{j2}\bar{Z}_6)]=q_{j1}m_j^2/v$
$G^+G^-h_j$	$v[q_{j1}Z_1+\mathrm{Re}(q_{j2}\bar{Z}_6)]=q_{j1}m_j^2/v$
$G^+H^-h_j$	$\frac{1}{2}v[q_{j2}Z_4+q_{j2}^*\bar{Z}_5^*+2q_{j1}\bar{Z}_6^*]=q_{j2}(m_j^2-m_{H^\pm}^2)/v$
$G^-H^+h_j$	$\frac{1}{2}v[q_{j2}^*Z_4+q_{j2}\bar{Z}_5+2q_{j1}\bar{Z}_6]=q_{j2}^*(m_j^2-m_{H^\pm}^2)/v$
$H^+H^-h_j$	$v[q_{j1}Z_3+\mathrm{Re}(q_{j2}\bar{Z}_7)]$
$h_jh_jh_j$	$3v[q_{j1}^3Z_1+q_{j1}\lvert q_{j2}\rvert^2Z_{34}+q_{j1}\mathrm{Re}(q_{j2}^2\bar{Z}_5)+3q_{j1}^2\mathrm{Re}(q_{j2}\bar{Z}_6)+\lvert q_{j2}\rvert^2\mathrm{Re}(q_{j2}\bar{Z}_7)]$
$h_jh_jh_k$	$v\{3q_{j1}^2q_{k1}Z_1+[q_{k1}\lvert q_{j2}\rvert^2+2q_{j1}\mathrm{Re}(q_{j2}q_{k2}^*)]Z_{34}+2q_{j1}\mathrm{Re}(q_{j2}q_{k2}\bar{Z}_5)+q_{k1}\mathrm{Re}(q_{j2}^2\bar{Z}_5)+3q_{j1}^2\mathrm{Re}(q_{k2}\bar{Z}_6)+6q_{j1}q_{k1}\mathrm{Re}(q_{j2}\bar{Z}_6)$ $+2\lvert q_{j2}\rvert^2\mathrm{Re}(q_{k2}\bar{Z}_7)+\mathrm{Re}(q_{k2}^*q_{j2}^2\bar{Z}_7)\}$
$h_jh_kh_\ell$	$v\{3q_{j1}q_{k1}q_{\ell 1}Z_1+[q_{j1}\mathrm{Re}(q_{k2}q_{\ell 2}^*)+q_{k1}\mathrm{Re}(q_{j2}q_{\ell 2}^*)+q_{\ell 1}\mathrm{Re}(q_{j2}q_{k2}^*)]Z_{34}+q_{j1}\mathrm{Re}(q_{k2}q_{\ell 2}\bar{Z}_5)+q_{k1}\mathrm{Re}(q_{j2}q_{\ell 2}\bar{Z}_5)$ $+q_{\ell 1}\mathrm{Re}(q_{j2}q_{k2}\bar{Z}_5)+3q_{j1}q_{k1}\mathrm{Re}(q_{\ell 2}\bar{Z}_6)+3q_{j1}q_{\ell 1}\mathrm{Re}(q_{k2}\bar{Z}_6)+3q_{k1}q_{\ell 1}\mathrm{Re}(q_{j2}\bar{Z}_6)+\mathrm{Re}(q_{j2}^*q_{k2}q_{\ell 2}\bar{Z}_7)$ $+\mathrm{Re}(q_{j2}q_{k2}^*q_{\ell 2}\bar{Z}_7)+\mathrm{Re}(q_{j2}q_{k2}q_{\ell 2}^*\bar{Z}_7)\}$

In the case of a CP-conserving Higgs scalar potential and vacuum, eq. (6) is satisfied, and the above results simplify significantly. In particular, one can fix the Higgs basis up to a potential sign ambiguity by choosing the phase $e^{-i\eta}$ such that Y_3, Z_5, Z_6, and Z_7 are all simultaneously real, which yields the so-called real Higgs basis (after absorbing the phase into the definition of the Higgs basis fields). The remaining ambiguity in defining the real Higgs basis is due to the possibility of transforming $\mathcal{H}_2 \to -\mathcal{H}_2$, in which case Y_3, Z_6, and Z_7 change sign (whereas all other scalar potential parameters in the real Higgs basis, including Z_5, are unchanged. Thus, it is convenient to define $\varepsilon \equiv e^{i\eta}$, where ε changes sign under $\mathcal{H}_2 \to -\mathcal{H}_2$. Following Refs. [105,106], we set $s_{13}=0$, $c_{13}=1$ and[24]

$$\varepsilon \equiv e^{i\eta} = \begin{cases} \mathrm{sgn}Z_6, & \text{if } Z_6 \neq 0, \\ \mathrm{sgn}Z_7, & \text{if } Z_6 = 0 \text{ and } Z_7 \neq 0. \end{cases} \tag{A40}$$

In the standard notation of the CP-conserving 2HDM, one chooses a real Φ-basis and defines $\tan\beta \equiv \langle\Phi_2^0\rangle/\langle\Phi_1^0\rangle$. The corresponding mixing angle that diagonalizes the CP-even Higgs squared-mass matrix is denoted by α. The CP-even scalar mass-eigenstates, h and H (with $m_h \leq m_H$), and the CP-odd scalar A are related to the neutral fields of the Higgs basis via

$$\begin{pmatrix} H \\ h \end{pmatrix} = \begin{pmatrix} c_{\beta-\alpha} & -s_{\beta-\alpha} \\ s_{\beta-\alpha} & c_{\beta-\alpha} \end{pmatrix} \begin{pmatrix} \sqrt{2}\mathrm{Re}H_1^0 - v \\ \sqrt{2}\mathrm{Re}H_2^0 \end{pmatrix}, \quad A = \sqrt{2}\mathrm{Im}H_2^0. \tag{A41}$$

where $c_{\beta-\alpha} \equiv \cos(\beta-\alpha)$ and $s_{\beta-\alpha} \equiv \sin(\beta-\alpha)$.

[24]If $Z_6 = Z_7 = 0$, then the sign of Z_5 is no longer invariant with respect to transformations that preserve the real Higgs basis (since the sign of Z_5 changes under $\mathcal{H}_2 \to \pm i\mathcal{H}_2$). In this case, it would be more appropriate to define $\varepsilon \equiv e^{2i\eta} = \mathrm{sgn}Z_5$.

Under the assumption that the lighter of the two neutral CP-even Higgs bosons is SM-like, it is convenient to make the following identifications:

$$h = h_1, \qquad H = -\varepsilon h_2, \qquad A = \varepsilon h_3. \tag{A42}$$

In light of eq. (A41), one can then identify

$$c_{12} = s_{\beta-\alpha}, \qquad s_{12} = -\varepsilon c_{\beta-\alpha}, \tag{A43}$$

where $0 \leq s_{\beta-\alpha} \leq 1$, and the q_{kj} of Table IV simplify to the results given in Table VI(a).[25]

If we examine the Higgs couplings to vector bosons and the Higgs boson self-couplings in the CP-conserving limit, we find that the following interactions that were originally present are now absent[26]:

$$\begin{aligned} &W^+W^-A, \quad ZZA, \quad ZHh, \quad hhA, \\ &hHA, \quad HHA, \quad H^+H^-A, \end{aligned} \tag{A44}$$

$$\begin{aligned} &hhhA, \quad hhHA, \quad hHHA, \quad HHHA, \\ &hAAA, \quad HAAA, \quad hAH^+H^-, \quad HAH^+H^-. \end{aligned} \tag{A45}$$

[25]Note that the signs of the fields H and A and the sign of $c_{\beta-\alpha}$ all flip under the redefinition of the Higgs basis field $\mathcal{H}_2 \to -\mathcal{H}_2$. In the CP-conserving 2HDM literature, in models in which the choice of the Φ_1–Φ_2 basis is physically meaningful (e.g., due to the presence of a discrete $\mathbb{Z}_2$ symmetry of the scalar potential), it is traditional to impose one further restriction that $\tan\beta$ is real and positive. This removes the final sign ambiguity in defining the real Higgs basis.

[26]Due to Bose symmetry, the couplings Zh_ih_i are absent in eq. (A38). Hence, in the CP-conserving limit, this means that the couplings Zhh, ZHH, and ZAA are absent.

TABLE VI. Invariant combinations q_{kj} defined in Table IV in the CP-conserving limit, corresponding to a real Higgs basis where $\varepsilon \equiv e^{i\eta}$ is given by eq. (A40). If the lighter of the two CP-even neutral scalars, h, is SM-like, then it is convenient to identify the h_k as shown in Table VI(a). If the heavier of the two CP-even neutral scalars, H, is SM-like, then it is convenient to identify the h_k as shown in Table VI(b).

(a) h is SM-like when $|c_{\beta-\alpha}| \ll 1$

k	h_k	q_{k1}	q_{k2}
1	h	$s_{\beta-\alpha}$	$\varepsilon c_{\beta-\alpha}$
2	$-\varepsilon H$	$-\varepsilon c_{\beta-\alpha}$	$s_{\beta-\alpha}$
3	εA	0	i

(b) H is SM-like when $|s_{\beta-\alpha}| \ll 1$

k	h_k	q_{k1}	q_{k2}
1	H	$c_{\beta-\alpha}$	$-\varepsilon s_{\beta-\alpha}$
2	εh	$\varepsilon s_{\beta-\alpha}$	$c_{\beta-\alpha}$
3	εA	0	i

TABLE VII. Nonvanishing cubic scalar self-couplings of the CP-conserving 2HDM involving the neutral and charged Goldstone fields. Charged fields point into the vertex. The interactions that do not appear in this table are zero after invoking the CP symmetry. See the caption to Table V.

Vertex	Self-coupling	In terms of masses
GhA	$v(Z_5 c_{\beta-\alpha} + Z_6 s_{\beta-\alpha})$	$[(m_h^2 - m_A^2)/v]c_{\beta-\alpha}$
GHA	$v(-Z_5 s_{\beta-\alpha} + Z_6 c_{\beta-\alpha})$	$-[(m_H^2 - m_A^2)/v]s_{\beta-\alpha}$
GGh	$v(Z_1 s_{\beta-\alpha} + Z_6 c_{\beta-\alpha})$	$(m_h^2/v)s_{\beta-\alpha}$
GGH	$v(Z_1 c_{\beta-\alpha} - Z_6 s_{\beta-\alpha})$	$(m_H^2/v)c_{\beta-\alpha}$
G^+G^-h	$v(Z_1 s_{\beta-\alpha} + Z_6 c_{\beta-\alpha})$	$(m_h^2/v)s_{\beta-\alpha}$
G^+G^-H	$v(Z_1 c_{\beta-\alpha} - Z_6 s_{\beta-\alpha})$	$(m_H^2/v)c_{\beta-\alpha}$
$G^\pm H^\mp h$	$v[\frac{1}{2}(Z_4 + Z_5)c_{\beta-\alpha} + Z_6 s_{\beta-\alpha}]$	$-[(m_{H^\pm}^2 - m_h^2)/v]c_{\beta-\alpha}$
$G^\pm H^\mp H$	$v[-\frac{1}{2}(Z_4 + Z_5)s_{\beta-\alpha} + Z_6 c_{\beta-\alpha}]$	$[(m_{H^\pm}^2 - m_H^2)/v]s_{\beta-\alpha}$
$G^\pm H^\mp A$	$\mp \frac{1}{2} i v(Z_5 - Z_4)$	$\mp i(m_{H^\pm}^2 - m_A^2)/v$

The cubic scalar couplings that are nonvanishing in the CP conserving limit are exhibited in Tables VII and VIII.

For completeness, we note that, under the assumption that the heavier of the two neutral CP-even Higgs bosons is SM-like, it is more convenient to replace the identifications previously made in eq. (A42) as follows:

$$H = h_1, \qquad h = \varepsilon h_2, \qquad A = \varepsilon h_3. \tag{A46}$$

In this case, the identifications given in eq. (A43) are replaced by

$$c_{12} = c_{\beta-\alpha}, \qquad s_{12} = \varepsilon s_{\beta-\alpha}, \tag{A47}$$

where $0 \le c_{\beta-\alpha} \le 1$, and the q_{kj} of Table IV simplify to the results given in Table VI(b). Note that the cubic scalar couplings exhibited in Tables VII and VIII remain unchanged.

5. 2HDM Yukawa couplings

Given the most general Yukawa Lagrangian involving the scalar fields of the 2HDM and the interaction eigenstate quark fields, one can derive expressions for the 3×3 complex up-type and down-type quark mass matrices by setting the neutral Higgs fields to their vacuum expectation values. Each of the two quark mass matrices can then be diagonalized via singular value decomposition, which yields a pair of unitary matrices that are then employed in defining the left-handed and right-handed quark mass-eigenstate fields, respectively.

After determining the quark mass eigenstate fields and the Higgs mass eigenstate fields, the resulting 2HDM Yukawa couplings in their most general form are (cf. eq. (58) of Ref. [104])

TABLE VIII. Nonvanishing cubic scalar of the CP-conserving 2HDM involving the physical scalar fields. We denote $Z_{34} \equiv Z_3 + Z_4$ and $Z_{345} \equiv Z_{34} + Z_5$. The interactions that do not appear in this table are zero after invoking the CP symmetry. See the caption to Table V.

Vertex	Self-coupling
hAA	$v[(Z_{34} - Z_5)s_{\beta-\alpha} + Z_7 c_{\beta-\alpha}]$
HAA	$v[(Z_{34} - Z_5)c_{\beta-\alpha} - Z_7 s_{\beta-\alpha}]$
hHH	$3v[Z_1 s_{\beta-\alpha} c_{\beta-\alpha}^2 + Z_{345} s_{\beta-\alpha}(\frac{1}{3} - c_{\beta-\alpha}^2) + Z_6 c_{\beta-\alpha}(1 - 3s_{\beta-\alpha}^2) + Z_7 s_{\beta-\alpha}^2 c_{\beta-\alpha}]$
Hhh	$3v[Z_1 c_{\beta-\alpha} s_{\beta-\alpha}^2 + Z_{345} c_{\beta-\alpha}(\frac{1}{3} - s_{\beta-\alpha}^2) - Z_6 s_{\beta-\alpha}(1 - 3c_{\beta-\alpha}^2) - Z_7 c_{\beta-\alpha}^2 s_{\beta-\alpha}]$
hhh	$3v[Z_1 s_{\beta-\alpha}^3 + Z_{345} s_{\beta-\alpha} c_{\beta-\alpha}^2 + 3Z_6 c_{\beta-\alpha} s_{\beta-\alpha}^2 + Z_7 c_{\beta-\alpha}^3]$
HHH	$3v[Z_1 c_{\beta-\alpha}^3 + Z_{345} c_{\beta-\alpha} s_{\beta-\alpha}^2 - 3Z_6 s_{\beta-\alpha} c_{\beta-\alpha}^2 - Z_7 s_{\beta-\alpha}^3]$
hH^+H^-	$v(Z_3 s_{\beta-\alpha} + Z_7 c_{\beta-\alpha})$
HH^+H^-	$v(Z_3 c_{\beta-\alpha} - Z_7 s_{\beta-\alpha})$

$$-\mathcal{L}_Y = \frac{1}{v}\bar{D}\left\{q_{k1}M_D + \frac{v}{\sqrt{2}}[q_{k2}\rho^{D\dagger}P_R + q_{k2}^*\rho^D P_L]\right\}Dh_k + \frac{1}{v}\bar{U}\left\{q_{k1}M_U + \frac{v}{\sqrt{2}}[q_{k2}^*\rho^U P_R + q_{k2}\rho^{U\dagger}P_L]\right\}Uh_k$$
$$+\left\{\bar{U}[K\rho^{D\dagger}P_R - \rho^{U\dagger}KP_L]DH^+ + \frac{\sqrt{2}}{v}\bar{U}[KM_DP_R - M_UKP_L]DG^+ + \text{H.c.}\right\}, \tag{A48}$$

where there is an implicit sum over the index $k = 1, 2, 3$; $P_{R,L} \equiv \frac{1}{2}(1 \pm \gamma_5)$; K is the CKM matrix; the mass-eigenstate down-type and up-type quark fields are $D = (d, s, b)^\mathsf{T}$ and $U \equiv (u, c, t)^\mathsf{T}$, respectively; and M_U and M_D are the diagonal quark mass matrices,

$$M_U = \frac{v}{\sqrt{2}}\kappa^U = \text{diag}(m_u, m_c, m_t),$$
$$M_D = \frac{v}{\sqrt{2}}\kappa^{D\dagger} = \text{diag}(m_d, m_s, m_b). \tag{A49}$$

The matrices ρ^U and ρ^D are independent complex 3×3 matrices that are invariant with respect to scalar basis transformations.

It is convenient to rewrite the Higgs-quark Yukawa couplings in terms of the following three 3×3 Hermitian matrices,

$$\rho_R^F \equiv \frac{v}{2\sqrt{2}}M_F^{-1/2}(\rho^F + \rho^{F\dagger})M_F^{-1/2},$$
$$\rho_I^F \equiv \frac{v}{2\sqrt{2}i}M_F^{-1/2}(\rho^F - \rho^{F\dagger})M_F^{-1/2}, \tag{A50}$$

for $F = U, D$, where the M_F are the diagonal fermion mass matrices [cf. eq. (A49)] and the Yukawa coupling matrices are introduced in eq. (A48). Then, the Yukawa couplings take the form

$$-\mathcal{L}_Y = \frac{1}{v}\bar{U}\sum_{k=1}^{3}M_U^{1/2}\{q_{k1}\mathbb{1} + \text{Re}(q_{k2})[\rho_R^U + i\gamma_5\rho_I^U] + \text{Im}(q_{k2})[\rho_I^U - i\gamma_5\rho_R^U]\}M_U^{1/2}Uh_k$$
$$+\frac{1}{v}\bar{D}\sum_{k=1}^{3}M_D^{1/2}\{q_{k1}\mathbb{1} + \text{Re}(q_{k2})[\rho_R^D - i\gamma_5\rho_I^D] + \text{Im}(q_{k2})[\rho_I^D + i\gamma_5\rho_R^D]\}M_D^{1/2}Dh_k$$
$$+\frac{\sqrt{2}}{v}\{\bar{U}[KM_D^{1/2}(\rho_R^D - i\rho_I^D)M_D^{1/2}P_R - M_U^{1/2}(\rho_R^U - i\rho_I^U)M_U^{1/2}KP_L]DH^+ + \text{H.c.}\}, \tag{A51}$$

where $\mathbb{1}$ is the 3×3 identity matrix. If the off-diagonal elements of $\rho_{R,I}^F$ are unsuppressed, then tree-level Higgs-mediated flavor changing neutral currents (FCNCs) will be generated that are incompatible with the strong suppression of FCNCs observed in nature.[27]

The A2HDM posits that the Yukawa matrices κ^F and ρ^F [cf. eq. (A48)] are proportional at the electroweak scale [73].[28] In light of eq. (A49), $\kappa^F = \sqrt{2}M_F/v$ is diagonal. Thus, in the A2HDM, the ρ^F are likewise diagonal, which implies that tree-level Higgs-mediated FCNCs are absent. We define the *alignment parameters* a^F via

$$\rho^F = a^F\kappa^F, \quad \text{for } F = U, D, E, \tag{A52}$$

where the (potentially) complex numbers a^F are invariant under the rephasing of the Higgs basis field $\mathcal{H}_2 \to e^{i\chi}\mathcal{H}_2$. It follows from eq. (A50) that

$$\rho_R^F = (\text{Re}a^F)\mathbb{1}, \qquad \rho_I^F = (\text{Im}a^F)\mathbb{1}. \tag{A53}$$

Inserting the above results into eq. (A48), the Yukawa couplings take the following form:

[27]Equation (A51) is easily extended to include the Higgs boson couplings to leptons. Since neutrinos are massless in the two-Higgs doublet extension of the Standard Model, one simply replaces $D \to E = (e, \mu, \tau)^\mathsf{T}$ and $U \to N = (\nu_e, \nu_\mu, \nu_\tau)^\mathsf{T}$, with $M_E = \text{diag}(m_e, m_\mu, m_\tau)$ and $M_N = 0$ in eqs. (A48) and (A51).

[28]Generically, the flavor-aligned conditions imposed by the A2HDM are not stable under renormalization group running [106,107], except in special cases where the flavor-aligned Yukawa couplings are a consequence of a symmetry [108]. Indeed, any such special case can be identified as one of the four type-I, -II, -X, and -Y Higgs-fermion Yukawa couplings [109–111], whose corresponding symmetries are exhibited in Table IX.

$$-\mathcal{L}_Y = \frac{1}{v}\bar{U}M_U\sum_{k=1}^{3}(q_{k1} + q_{k2}^* a^U P_R + q_{k2} a^{U*} P_L)Uh_k + \frac{1}{v}\sum_{F=D,E}\left\{\bar{F}M_F\sum_{k=1}^{3}(q_{k1} + q_{k2}a^{F*}P_R + q_{k2}^* a^F P_L)Fh_k\right\}$$
$$+\frac{\sqrt{2}}{v}\{\bar{U}[a^{D*}KM_D P_R - a^{U*}M_U K P_L]DH^+ + a^{E*}\bar{N}M_E P_R E H^+ + \text{H.c.}\}. \tag{A54}$$

This form simplifies further if the neutral Higgs mass eigenstates are also states of definite CP. In this case, the corresponding Yukawa couplings are given by

$$-\mathcal{L}_Y = \frac{1}{v}\sum_{F=U,D,E}\bar{F}M_F\{s_{\beta-\alpha} + \varepsilon c_{\beta-\alpha}[\text{Re}a^F + i\eta^F \text{Im}a^F\gamma_5]\}Fh + \frac{1}{v}\sum_{F=U,D,E}\bar{F}M_F\{c_{\beta-\alpha} - \varepsilon s_{\beta-\alpha}[\text{Re}a^F + i\eta^F\text{Im}a^F\gamma_5]\}FH$$
$$+\frac{1}{v}\sum_{F=U,D,E}\bar{F}M_F\{\varepsilon[\text{Im}a^F - i\eta^F\text{Re}a^F\gamma_5]\}FA + \frac{\sqrt{2}}{v}\varepsilon\{\bar{U}[a^{D*}KM_D P_R - a^{U*}M_U K P_L]DH^+ + a^{E*}\bar{N}M_E P_R E H^+ + \text{H.c.}\}, \tag{A55}$$

where ε is defined in eq. (A40) and we have introduced the notation

$$\eta^F \equiv \begin{cases} +1 & \text{for } F = U, \\ -1 & \text{for } F = D, E. \end{cases} \tag{A56}$$

Special cases of the A2HDM arise if the flavor alignment is the consequence of a symmetry. For Yukawa couplings of type I, II, X, and Y [108–111], one imposes a $\mathbb{Z}_2$ symmetry on the dimension-4 terms of the Higgs Lagrangian in the Φ-basis, where the $\mathbb{Z}_2$ charges are exhibited in Table IX. In particular, the type-I and type-II 2HDMs (and likewise the type-X and type-Y 2HDMs[29]) are special cases of the A2HDM, where one can identify the corresponding complex alignment parameters as follows:

(1) type I: $a^U = a^D = a^E = e^{i(\xi+\eta)}\cot\beta$.

(2) type II: $a^U = e^{i(\xi+\eta)}\cot\beta$ and $a^D = a^E = -e^{i(\xi+\eta)}\tan\beta$.

In the CP-conserving limit, it is conventional to define the scalar potential in the Φ-basis such that $\lambda_6 = \lambda_7 = 0$ and $\xi = 0$. In this convention, the vacuum expectation values are real, and $\tan\beta$ is non-negative, in which case we can identify $e^{i(\xi+\eta)} = \varepsilon$. Inserting the type-I or type-II values of the flavor alignment parameters in eq. (A55), we see that the factors of ε cancel exactly, as they must since there is no remaining twofold ambiguity in defining the real Higgs basis once a convention has been adopted such that $\tan\beta$ is non-negative.

6. Higgs alignment limit

In the Higgs alignment limit, one of the neutral scalars, which we conventionally choose to be h_1, is identified as the observed SM-like Higgs boson. Consequently,

$$\frac{g_{h_1VV}}{g_{h_{\rm SM}VV}} = q_{11} = c_{12}c_{13} \simeq 1, \quad \text{where } V = W \text{ or } Z, \tag{A57}$$

which implies that $|s_{12}|$, $|s_{13}| \ll 1$. Thus, eqs. (A25) and (A26) yield

$$|s_{12}| \simeq \left|\frac{v^2\text{Re}\bar{Z}_6}{m_2^2 - m_1^2}\right| \ll 1, \tag{A58}$$

$$|s_{13}| \simeq \left|\frac{v^2\text{Im}\bar{Z}_6}{m_3^2 - m_1^2}\right| \ll 1. \tag{A59}$$

In light of eq. (A28), one additional small quantity characterizes the Higgs alignment limit,

$$|\text{Im}(\bar{Z}_5)| \simeq \left|\frac{2(m_2^2 - m_1^2)s_{12}s_{13}}{v^2}\right| \simeq \left|\frac{v^2\text{Im}\bar{Z}_6^2}{m_3^2 - m_1^2}\right| \ll 1. \tag{A60}$$

Hence, the conditions for approximate Higgs alignment are as follows:

(1) Higgs alignment via decoupling is achieved if m_2, $m_3 \gg m_1 \simeq 125$ GeV [under the assumption that Z_6 is at most an $\mathcal{O}(1)$ parameter]. That is, $Y_2 \gg v^2$.

TABLE IX. Four possible $\mathbb{Z}_2$ charge assignments for scalar and fermion fields. The $\mathbb{Z}_2$ symmetry is employed to constrain the Higgs-fermion Yukawa couplings, thereby implementing the conditions for the natural absence of tree-level Higgs-mediated FCNCs.

	Φ_1	Φ_2	U_R	D_R	E_R	U_L, D_L, N_L, E_L
Type I	+	−	−	−	−	+
Type II	+	−	−	+	+	+
Type X	+	−	−	−	+	+
Type Y	+	−	−	+	−	+

[29] In type-X models, the quarks possess type-I Yukawa couplings, whereas the leptons possess type-II Yukawa couplings. In type-Y models, the quarks possess type-II Yukawa couplings, whereas the leptons possess type-I Yukawa couplings.

(2) Approximate Higgs alignment without decoupling is achieved if $|Z_6| \ll 1$, while all Higgs squared masses are of $\mathcal{O}(v^2)$.[30]

We also obtain the following approximate mass relations,

$$m_1^2 \simeq v^2[Z_1 - s_{12}\mathrm{Re}\bar{Z}_6 + s_{13}\mathrm{Im}\bar{Z}_6], \tag{A61}$$

$$m_2^2 - m_3^2 \simeq v^2[\mathrm{Re}\bar{Z}_5 + s_{12}\mathrm{Re}\bar{Z}_6 + s_{13}\mathrm{Im}\bar{Z}_6], \tag{A62}$$

$$m_2^2 - m_{H^\pm}^2 \simeq \frac{1}{2}v^2[Z_4 + \mathrm{Re}\bar{Z}_5 + 2s_{12}\mathrm{Re}\bar{Z}_6], \tag{A63}$$

to first order in the deviation from exact Higgs alignment.

In the case of exact Higgs alignment, the SM-like Higgs boson resides entirely in the Higgs basis field $\mathcal{H}_1$; i.e., it is aligned in field space with the direction of the neutral Higgs vacuum expectation value. Thus, we can identify $h_1 = \sqrt{2}\mathrm{Re}\mathcal{H}_1^0 - v$. In this case, h_1 does not mix with the neutral scalar fields that reside in $\mathcal{H}_2$. In light of eq. (A13), it then follows that $Z_6 = 0$. However, a second condition arises in the diagonalization of the neutral scalar squared-mass matrix. We will demonstrate below that the conditions for exact Higgs alignment, where h_1 is identified with the SM Higgs boson, are given by

$$\mathrm{Im}\bar{Z}_5 = 0 \quad \text{and} \quad Z_6 = 0. \tag{A64}$$

In particular, in the exact Higgs alignment limit where eq. (A64) holds, $\mathcal{M}^2$ is a diagonal matrix, and we can immediately identify

$$m_1^2 = Z_1 v^2, \qquad m_{2,3}^2 = Y_2 + \frac{1}{2}v^2[Z_{34} \pm \mathrm{Re}\bar{Z}_5]. \tag{A65}$$

To understand the origin of the condition that $\mathrm{Im}\bar{Z}_5 = 0$, note that $c_{12} = c_{13} = 1$ in the exact Higgs alignment limit, or equivalently $R_{12} = R_{13} = \mathbb{1}_{3\times 3}$. Hence,

$$R\mathcal{M}_0^2 R^{\mathsf{T}} = R_{23}\mathcal{M}_0^2 R_{23}^{\mathsf{T}} = \mathrm{diag}(m_1^2, m_2^2, m_3^2), \tag{A66}$$

where

$$\mathcal{M}_0^2 = \begin{pmatrix} Z_1 v^2 & 0 & 0 \\ 0 & Y_2 + \frac{1}{2}v^2[Z_{34} + \mathrm{Re}\bar{Z}_5] & -\frac{1}{2}v^2\mathrm{Im}\bar{Z}_5 \\ 0 & -\frac{1}{2}v^2\mathrm{Im}\bar{Z}_5 & Y_2 + \frac{1}{2}v^2[Z_{34} - \mathrm{Re}\bar{Z}_5] \end{pmatrix} \tag{A67}$$

is the neutral scalar squared mass matrix in the exact Higgs alignment limit. But having rephased $\mathcal{H}_2$ to set $\theta_{23} = 0$ as discussed below eq. (A18), it follows that $R_{23} = \mathbb{1}_{3\times 3}$. Hence, eq. (A66) implies that $\mathcal{M}_0^2$ is a diagonal matrix, and we conclude that $\mathrm{Im}\bar{Z}_5 = 0$.

In the exact Higgs alignment limit where $Y_3 = Z_6 = 0$, the only potentially complex parameters of the scalar potential in the Higgs basis are Z_5 and Z_7. With the rephasing freedom exhibited in eq. (A30), we can assume that Z_5 is real without loss of generality. Thus, the only remaining potentially complex parameter in the scalar potential is Z_7. Since the neutral Higgs squared-mass matrix is independent of Z_7, it follows that Higgs boson–gauge boson interactions are separately *CP* conserving in the exact Higgs alignment limit. The scalar mass eigenstates can be identified as eigenstates of the diagonal squared-mass matrix $\mathcal{M}^2$, with squared masses

$$m_h^2 = Z_1 v^2, \qquad m_{H,A}^2 = Y_2 + \frac{1}{2}(Z_3 + Z_4 \pm Z_5). \tag{A68}$$

That is, the neutral scalar mass eigenstates are states of definite *CP*. The only potential source of *CP* violation resides in the Higgs self-interactions in the case of $\mathrm{Im}(Z_5^* Z_7^2) \neq 0$.

In this paper, we have proposed to make use of the $H^+H^-h_k$ interactions,

$$h_k H^+H^-:\ v[q_{k1}Z_3 + \mathrm{Re}(q_{k2}\bar{Z}_7)], \tag{A69}$$

where only *CP*-even states can couple to H^+H^- if *CP* is conserved. In the exact Higgs alignment limit, $q_{11} = 1$, $q_{21} = q_{31} = q_{12} = 0$, $q_{22} = 1$, and $q_{32} = i$. Thus, h_1 is *CP* even as anticipated. Assuming that $Z_7 \neq 0$, the $H^+H^-h_2$ coupling is nonvanishing if $\mathrm{Im}\bar{Z}_7 = 0$, whereas the

TABLE X. Cubic self-couplings of the physical Higgs scalars of the 2HDM in the approximate Higgs alignment limit without decoupling (where $|Z_6| \ll 1$). Charged fields point into the vertex. The first order corrections to the exact Higgs alignment limit, which are linear in s_{12}, s_{13}, and $\bar{Z}_6$, are exhibited.

Vertex	Self-coupling
$H^+H^-h_1$	$v[Z_3 - s_{12}\mathrm{Re}\bar{Z}_7 + s_{13}\mathrm{Im}\bar{Z}_7]$
$H^+H^-h_2$	$v[\mathrm{Re}\bar{Z}_7 + s_{12}Z_3]$
$H^+H^-h_3$	$-v[\mathrm{Im}\bar{Z}_7 - s_{13}Z_3]$
$h_1h_1h_1$	$3vZ_1$
$h_2h_2h_2$	$3v[\mathrm{Re}\bar{Z}_7 + s_{12}(Z_{34} + \mathrm{Re}\bar{Z}_5)]$
$h_3h_3h_3$	$-3v[\mathrm{Im}\bar{Z}_7 - s_{13}(Z_{34} - \mathrm{Re}\bar{Z}_5)]$
$h_1h_2h_2$	$v[Z_{34} + \mathrm{Re}\bar{Z}_5 - 3s_{12}\mathrm{Re}\bar{Z}_7 + s_{13}\mathrm{Im}\bar{Z}_7]$
$h_1h_3h_3$	$v[Z_{34} - \mathrm{Re}\bar{Z}_5 - s_{12}\mathrm{Re}\bar{Z}_7 + 3s_{13}\mathrm{Im}\bar{Z}_7]$
$h_2h_1h_1$	$v[s_{12}(3Z_1 - 2Z_{34} - 2\mathrm{Re}\bar{Z}_5) + 3\mathrm{Re}\bar{Z}_6]$
$h_2h_3h_3$	$v[\mathrm{Re}\bar{Z}_7 + s_{12}(Z_{34} - \mathrm{Re}\bar{Z}_5)]$
$h_3h_1h_1$	$v[s_{13}(3Z_1 - 2Z_{34} + 2\mathrm{Re}\bar{Z}_5) - 3\mathrm{Im}\bar{Z}_6]$
$h_3h_2h_2$	$-v[\mathrm{Im}\bar{Z}_7 - s_{13}(Z_{34} + \mathrm{Re}\bar{Z}_5)]$
$h_1h_2h_3$	$-v[s_{13}\mathrm{Re}\bar{Z}_7 - s_{12}\mathrm{Im}\bar{Z}_7]$

[30]More precisely, we require that $|Z_6| \ll \Delta m_{j1}^2/v^2$, where $\Delta m_{j1}^2 \equiv m_j^2 - m_1^2$ for $j = 2, 3$.

$H^+H^-h_3$ coupling is nonvanishing if $\mathrm{Re}\bar{Z}_7 = 0$. Thus, we again conclude (as previously noted in Table II) that if $Z_7 \neq 0$, then

$$\mathrm{Im}\bar{Z}_7 = 0 \Rightarrow h_2 \text{ is } CP \text{ even and } h_3 \text{ is } CP \text{ odd},$$
$$\mathrm{Re}\bar{Z}_7 = 0 \Rightarrow h_2 \text{ is } CP \text{ odd and } h_3 \text{ is } CP \text{ even}. \tag{A70}$$

For more details, see Appendix C of Ref. [112].

In light of the precision LHC Higgs data, the departure from the exact Higgs alignment limit is expected to be small. Thus, it is useful to exhibit the Higgs couplings in the approximate Higgs alignment limit, where only terms that are first order in the small parameters that govern the Higgs alignment limit are kept, as shown in Table X. Here, one must distinguish between the Higgs alignment limit without decoupling, where $|Z_6| \ll 1$, and the decoupling limit where $|s_{12}|$, $|s_{13}|$, $|\mathrm{Im}\bar{Z}_5| \ll 1$ by virtue of the fact that m_2, $m_3 \gg v$. In this paper, our phenomenological considerations are based on the assumption that the masses of h_2 and h_3 are not significantly larger than $\mathcal{O}(v)$. As a result, we assume that $\bar{Z}_6$ is sufficiently suppressed to be consistent with the observed SM-like Higgs boson h_1. In particular, the cubic self-couplings of the physical Higgs scalars of the 2HDM are given in Table X in the approximate Higgs alignment limit without decoupling, where $|Z_6| \ll 1$. The first order corrections to the exact Higgs alignment results shown in Table X are linear in s_{12}, s_{13}, and $\bar{Z}_6$. Note that in the approximate Higgs alignment limit without decoupling, $\mathrm{Im}\bar{Z}_5 \sim \mathcal{O}(|Z_6|^2)$ is a second order effect and hence can be neglected [cf. eq. (A60)].

Finally, we record the structure of the neutral Higgs-quark Yukawa couplings of the A2HDM in the exact Higgs alignment limit. Inserting the values for the q_{kj} given below eq. (A69) into eq. (A54), we end up with

$$-\mathcal{L} = \frac{1}{v}(\bar{U}M_U U + \bar{D}M_D D + \bar{E}M_E E)h_1 + \frac{1}{v}\left[\bar{U}M_U(\mathrm{Re}a^U + i\gamma_5 \mathrm{Im}a^U)U + \sum_{F=D,E} \bar{F}M_F(\mathrm{Re}a^F - i\gamma_5 \mathrm{Im}a^F)F\right]h_2$$
$$+\frac{1}{v}\left[\bar{U}M_U(\mathrm{Im}a^U - i\gamma_5 \mathrm{Re}a^U)U + \sum_{F=D,E} \bar{F}M_F(\mathrm{Im}a^F + i\gamma_5 \mathrm{Re}a^F)F\right]h_3. \tag{A71}$$

As expected, in the limit of exact Higgs alignment, the Yukawa couplings of h_1 coincide with those of the SM Higgs boson.

APPENDIX B: PROCESSES WITH AN ODD NUMBER OF PHOTONS

Consider 2HDM processes involving bosonic external states in the limit of exact Higgs alignment (where the Yukawa interactions, which can contribute via fermionic loops, are neglected). If the scalar potential is CP conserving, then $\mathrm{Re}\bar{Z}_7\mathrm{Im}\bar{Z}_7 = 0$ [cf. eq. (9)], and the bosonic sector separately conserves C and P, with assigned quantum numbers as indicated in Table I. For definiteness, we henceforth assume that $\mathrm{Im}\bar{Z}_7 = 0$, in which case we can identify $h_2 = H$ and $h_3 = A$.[31]

Under the conditions elucidated above, we expect the process $h_2 \to \gamma\gamma\gamma$ to be absent, since the initial state (h_2) is C even and the final state ($\gamma\gamma\gamma$) is C odd. In contrast, the process $h_3 \to \gamma\gamma\gamma$ is allowed, because h_3 is C odd. At the one-loop level, the Feynman diagrams for both processes have identical topologies: (a) the box topology with an internal charged Higgs boson and three $H^+H^-\gamma$ vertices and (b) the triangle topology with an internal charged Higgs boson that contains a $H^+H^-\gamma$ and a $H^+H^-\gamma\gamma$ vertex. Representative diagrams for these topologies are depicted in Fig. 9 (there are also four additional box diagrams corresponding to the other four possible permutations of the external photon lines). The only difference between the one-loop decay matrix elements for the processes $h_2 \to \gamma\gamma\gamma$ and $h_3 \to \gamma\gamma\gamma$ at the one-loop level is the appearance of the

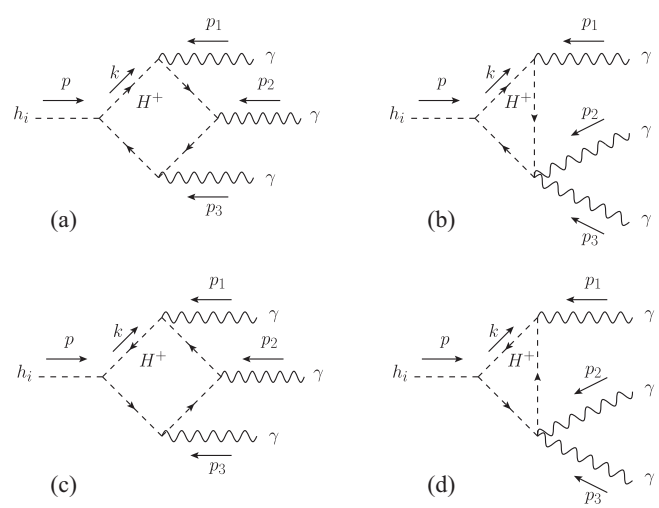

FIG. 9. Representative box diagrams [graphs (a) and (c)] and triangle diagrams [graphs (b) and (d)] with an internal charged Higgs boson, $H^\pm$, for the $h_i \to \gamma\gamma\gamma$ ($i = 2, 3$) process. The arrows on the charged Higgs propagator denote the flow of electric charge.

[31] If one were to assume that $\mathrm{Re}\bar{Z}_7 = 0$, then simply interchange h_2 and h_3 in the discussion above (in light of Table II).

different coupling factors of the $h_2H^+H^-$ and $h_3H^+H^-$ vertices, respectively. In particular, these coupling factors are just numbers (independent of momenta). Hence, it follows that if the one-loop matrix element for $h_2 \to \gamma\gamma\gamma$ vanishes due to the C and P invariance of the 2HDM bosonic sector, then the one-loop matrix element for $h_3 \to \gamma\gamma\gamma$ must vanish as well (despite the fact that $h_3 \to \gamma\gamma\gamma$ is allowed by C and P invariance).

Indeed, it is easy to see that the sum of the one-loop diagrams that contribute to $h_i \to \gamma\gamma\gamma$ vanishes. In Fig. 9(a), each $H^+H^-\gamma$ vertex gives rise to a factor $-ieq_j^\mu$, where $j = 1,\ 2,\ 3$ enumerates the momenta of the external photons, and the momenta q_j^μ are

$$\begin{aligned} q_1^\mu &= 2k + p_1, \\ q_2^\mu &= 2k + 2p_1 + p_2, \\ q_3^\mu &= 2k + 2p_1 + 2p_2 + p_3. \end{aligned} \tag{B1}$$

In contrast, due to the reversed flow of electric charge in the loop, each vertex in Fig. 9(c) gives a contribution of $+ieq_j^\mu$, whereas everything else (assignment of momenta, etc.) is identical to Fig. 9(a). Thus, with an odd number of $H^+H^-\gamma$ vertices, these two contributions cancel. The same can be observed between the diagrams in Figs. 9(b) and 9(d), where the $H^+H^-\gamma$ vertex gives $-iep_j^\mu$ in diagram (b) and $+iep_j^\mu$ in diagram (d), and the $H^+H^-\gamma\gamma$ vertex in both cases simply gives a factor of $2ie^2$.

If we now allow for CP-violating interactions in the scalar potential, then $\mathrm{Re}\bar{Z}_7\mathrm{Im}\bar{Z}_7 \neq 0$ [cf. eq. (9)], in which case both the $h_2H^+H^-$ and $h_3H^+H^-$ vertices exist. Nevertheless, the sum of the one-loop diagrams that contribute to $h_i \to \gamma\gamma\gamma$ still vanishes since the cancellation of diagrams is not affected by the value of the $h_iH^+H^-$ coupling.

The sum of the one-loop contributions in which the internal $H^\pm$ is replaced by the $W^\pm$ must also vanish if C and P are separately conserved, since the W^+W^- system in a total angular momentum zero state has $C = P = +1$. Hence, $h_i \to W^+W^- \to \gamma\gamma\gamma$ (via the one-loop diagrams with topologies exhibited in Fig. 9) for any scalar h_i is forbidden by the C invariance of the 2HDM bosonic sector. If h_2 and h_3 are CP-mixed states, then the vanishing of the corresponding one-loop matrix element is again unchanged. Once again, this conclusion can be verified diagrammatically by explicitly exhibiting the cancellation among diagrams by repeating the analysis used above for the $H^\pm$ loop.

Although the bosonic contributions to the one-loop matrix element for the C-conserving, P-conserving $h_3 \to \gamma\gamma\gamma$ decay vanish, the cancellation does not persist at two loops. Two possible diagrams that occur at the two-loop level and contribute to $h_3 \to \gamma\gamma\gamma$ are depicted in Fig. 10. This decay can be described by an effective Lagrangian [113–115],

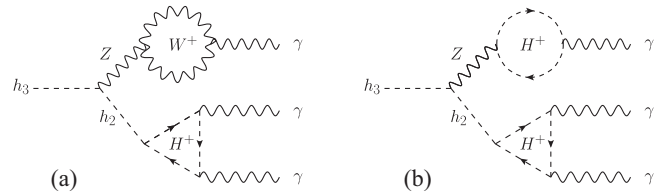

FIG. 10. Sample diagrams for two-loop contributions to the decay process $h_3 \to \gamma\gamma\gamma$.

$$\mathcal{L}_{\mathrm{eff}} = \frac{\kappa_3}{\Lambda^7} h_3(\partial^\beta F_{\sigma\tau})(\partial_\rho F_{\alpha\beta})(\partial^\rho\partial^\alpha F_{\sigma\tau}), \tag{B2}$$

where $F_{\mu\nu}$ is the electromagnetic field strength tensor, κ_3 is dimensionless, and Λ is a parameter with dimensions of mass. The corresponding decay amplitude in terms of form factors is given in Ref. [116]. In contrast, the analogous diagrams for the C-violating, P-conserving $h_2 \to \gamma\gamma\gamma$ decay (obtained by interchanging h_2 and h_3 in Fig. 10) require a nonvanishing $h_3H^+H^-$ coupling, i.e., $\mathrm{Im}\bar{Z}_7 \neq 0$. Hence, the matrix element for the process $h_2 \to \gamma\gamma\gamma$ is proportional to a bosonic P-even, CP-violating coupling, as expected.

Finally, consider how the above results are modified when the Yukawa couplings are taken into account. At one-loop order, new diagrams must be considered with the topology of Figs. 9(a) and 9(c), where the H^+ is replaced by a fermion. Thus, to analyze these contributions, we can consider a subset of the 2HDM fields that contains the neutral scalars $h_{1,2,3}$, the fermions, and the photon (but with the $W^\pm$, Z, and $H^\pm$ removed). In this truncated theory, if the scalar potential is CP conserving, then C and P are separately conserved. However, the J^{PC} quantum numbers of the scalars are $h_1(0^{++})$, $h_2(0^{++})$, and $h_3(0^{-+})$. Note that the J^{PC} assignment for h_3 is different than the 0^{+-} assignment that appears in Table I. Moreover, if the scalar potential is CP violating, then the truncated theory remains C conserving since $\bar{\psi}\psi$ and $\bar{\psi}\gamma_5\psi$ are both $C = +1$ bilinears. It immediately follows that the one-loop amplitude for $h_i \to \gamma\gamma\gamma$ vanishes due to C invariance (otherwise known as Furry's theorem).

At two-loop order, one can no longer assign a unique C quantum number to h_3. That is, in the 2HDM coupled to the complete electroweak sector, if the scalar potential is CP conserving, then h_2 is CP even, and h_3 is CP odd, but C and P are no longer separately conserved.[32] For example, if we consider the two-loop diagrams of Fig. 10, where the H^+ loop in the triangle subgraph is replaced by a fermion, and the corresponding graph where h_2 and h_3 are interchanged, then the contributions to the two-loop amplitudes for $h_{2,3} \to \gamma\gamma\gamma$ are nonzero. In other words, there exist both CP-even and CP-odd effective operators involving three

[32]Ultimately, one expects to find the effects of CP violation to leak into the scalar sector due to the CKM phase in the Yukawa interactions. However, such effects are highly suppressed and will not enter until at least four-loop order [117].

photon field strength tensors that can couple to an external scalar field [114,115]. The CP-conserving effective Lagrangian that governs the $h_{2,3} \to \gamma\gamma\gamma$ decays is

$$\mathcal{L}_{\rm eff} = \frac{1}{\Lambda^7}[\kappa_2 h_2 \partial^\beta \tilde{F}_{\sigma\tau} + \kappa_3 h_3 \partial^\beta F^{\sigma\tau}](\partial_\rho F_{\alpha\beta})(\partial^\rho \partial^\alpha F_{\sigma\tau}), \quad \text{(B3)}$$

where $\tilde{F}_{\sigma\tau} \equiv \frac{1}{2}\epsilon_{\mu\nu\sigma\tau}F^{\mu\nu}$ is the dual electromagnetic field strength tensor and $\kappa_{2,3}$ are dimensionless parameters. In particular, if the scalar sector is CP conserving, then both decays $h_{2,3} \to \gamma\gamma\gamma$ are allowed. The term in the effective Lagrangian involving the dual electromagnetic field strength tensor arises due to the γ_5 that appears in the $h_3\bar{\psi}\gamma_5\psi$ coupling. This is in contrast to the behavior of the bosonic sector in isolation, where $h_2 \to \gamma\gamma\gamma$ can be interpreted as a signal of a P-even, CP-violating interaction, since in this case there is no way to generate $\kappa_2 \neq 0$ via diagrams that involve only bosonic fields.

[1] J. F. Gunion, H. E. Haber, G. L. Kane, and S. Dawson, *The Higgs Hunter's Guide* (Westview Press, Boulder, CO, 2000).
[2] The ATLAS Collaboration, Nature (London) **607**, 52 (2022).
[3] The CMS Collaboration, Nature (London) **607**, 60 (2022).
[4] I. F. Ginzburg, M. Krawczyk, and P. Osland, Nucl. Instrum. Methods Phys. Res., Sect. A **472**, 149 (2001).
[5] J. F. Gunion and H. E. Haber, Phys. Rev. D **67**, 075019 (2003).
[6] N. Craig, J. Galloway, and S. Thomas, arXiv:1305.2424.
[7] D. M. Asner, T. Barklow, C. Calancha, K. Fujii, N. Graf, H. E. Haber, A. Ishikawa, S. Kanemura, S. Kawada, M. Kurata *et al.*, arXiv:1310.0763, contribution to the Proceedings of the Community Summer Study 2013: Snowmass on the Mississippi.
[8] M. Carena, I. Low, N. R. Shah, and C. E. M. Wagner, J. High Energy Phys. 04 (2014) 015.
[9] H. E. Haber, in *Proceedings of the Toyama International Workshop on Higgs as a Probe of New Physics 2013 (HPNP2013)* (2013), arXiv:1401.0152.
[10] H. Georgi and D. V. Nanopoulos, Phys. Lett. **82B**, 95 (1979).
[11] L. Lavoura, Phys. Rev. D **50**, 7089 (1994).
[12] L. Lavoura and J. P. Silva, Phys. Rev. D **50**, 4619 (1994).
[13] F. J. Botella and J. P. Silva, Phys. Rev. D **51**, 3870 (1995).
[14] G. C. Branco, L. Lavoura, and J. P. Silva, *CP Violation* (Oxford University Press, Oxford, UK, 1999).
[15] S. Davidson and H. E. Haber, Phys. Rev. D **72**, 035004 (2005); **72**, 099902(E) (2005).
[16] H. E. Haber and Y. Nir, Nucl. Phys. **B335**, 363 (1990).
[17] P. S. Bhupal Dev and A. Pilaftsis, J. High Energy Phys. 12 (2014) 024; 11 (2015) 147(E).
[18] P. S. Bhupal Dev and A. Pilaftsis, J. Phys. Conf. Ser. **873**, 012008 (2017).
[19] K. Benakli, M. D. Goodsell, and S. L. Williamson, Eur. Phys. J. C **78**, 658 (2018).
[20] K. Lane and W. Shepherd, Phys. Rev. D **99**, 055015 (2019).
[21] K. Benakli, Y. Chen, and G. Lafforgue-Marmet, Eur. Phys. J. C **79**, 172 (2019).
[22] N. Darvishi and A. Pilaftsis, Proc. Sci., CORFU2019 (**2020**) 064.
[23] P. Draper, A. Ekstedt, and H. E. Haber, J. High Energy Phys. 05 (2021) 235.
[24] E. J. Eichten and K. Lane, Phys. Rev. D **103**, 115022 (2021).
[25] R. Barbieri, L. J. Hall, and V. S. Rychkov, Phys. Rev. D **74**, 015007 (2006).
[26] L. Lopez Honorez, E. Nezri, J. F. Oliver, and M. H. G. Tytgat, J. Cosmol. Astropart. Phys. 02 (2007) 028.
[27] B. Grzadkowski, O. M. Ogreid, P. Osland, A. Pukhov, and M. Purmohammadi, J. High Energy Phys. 06 (2011) 003.
[28] I. P. Ivanov and V. Keus, Phys. Rev. D **86**, 016004 (2012).
[29] V. Keus, S. F. King, S. Moretti, and D. Sokolowska, J. High Energy Phys. 11 (2014) 016.
[30] V. Keus, S. F. King, and S. Moretti, Phys. Rev. D **90**, 075015 (2014).
[31] A. Cordero-Cid, J. Hernández-Sánchez, V. Keus, S. F. King, S. Moretti, D. Rojas, and D. Sokołowska, J. High Energy Phys. 12 (2016) 014.
[32] D. Azevedo, P. M. Ferreira, M. M. Muhlleitner, S. Patel, R. Santos, and J. Wittbrodt, J. High Energy Phys. 11 (2018) 091.
[33] A. Aranda, D. Hernández-Otero, J. Hernández-Sanchez, V. Keus, S. Moretti, D. Rojas-Ciofalo, and T. Shindou, Phys. Rev. D **103**, 015023 (2021).
[34] W. Khater, A. Kunčinas, O. M. Ogreid, P. Osland, and M. N. Rebelo, J. High Energy Phys. 01 (2022) 120.
[35] J. F. Gunion, H. E. Haber, and J. Wudka, Phys. Rev. D **43**, 904 (1991).
[36] B. Grzadkowski and J. F. Gunion, Phys. Lett. B **294**, 361 (1992).
[37] B. Grzadkowski and J. F. Gunion, Phys. Lett. B **350**, 218 (1995).
[38] W. Bernreuther, A. Brandenburg, and M. Flesch, Phys. Rev. D **56**, 90 (1997).
[39] S. Berge, W. Bernreuther, B. Niepelt, and H. Spiesberger, Phys. Rev. D **84**, 116003 (2011).
[40] S. Berge, W. Bernreuther, and S. Kirchner, Eur. Phys. J. C **74**, 3164 (2014).
[41] A. Cordero-Cid, J. Hernández-Sánchez, V. Keus, S. Moretti, D. Rojas-Ciofalo, and D. Sokołowska, Phys. Rev. D **101**, 095023 (2020).
[42] J. F. Gunion and X. G. He, Phys. Rev. Lett. **76**, 4468 (1996).
[43] F. Boudjema, R. M. Godbole, D. Guadagnoli, and K. A. Mohan, Phys. Rev. D **92**, 015019 (2015).

[44] N. Mileo, K. Kiers, A. Szynkman, D. Crane, and E. Gegner, J. High Energy Phys. 07 (2016) 056.
[45] S. Amor dos Santos, M. C. N. Fiolhais, R. Frederix, R. Gonçalo, E. Gouveia, R. Martins, A. Onofre, C. M. Pease, H. Peixoto, A. Reigoto, R. Santos, and J. Silva, Phys. Rev. D **96**, 013004 (2017).
[46] D. Gonçalves, K. Kong, and J. H. Kim, J. High Energy Phys. 06 (2018) 079.
[47] A. M. Sirunyan *et al.* (CMS Collaboration), Phys. Rev. Lett. **125**, 061801 (2020).
[48] G. Aad *et al.* (ATLAS Collaboration), Phys. Rev. Lett. **125**, 061802 (2020).
[49] A. Tumasyan *et al.* (CMS Collaboration), J. High Energy Phys. 06 (2022) 012.
[50] A. Mendez and A. Pomarol, Phys. Lett. B **272**, 313 (1991).
[51] G. Cvetic, M. Nowakowski, and A. Pilaftsis, Phys. Lett. B **301**, 77 (1993).
[52] D. Fontes, J. C. Romão, R. Santos, and J. P. Silva, Phys. Rev. D **92**, 055014 (2015).
[53] V. Keus, S. F. King, S. Moretti, and K. Yagyu, J. High Energy Phys. 04 (2016) 048.
[54] D. de Florian *et al.* (LHC Higgs Cross Section Working Group), *Handbook of LHC Higgs Cross Sections: 4. Deciphering the Nature of the Higgs Sector*, CERN Yellow Reports: Monographs Vol. 2 (CERN, Geneva, 2017), 10.23731/CYRM-2017-002.
[55] H. Abouabid, A. Arhrib, D. Azevedo, J. E. Falaki, P. M. Ferreira, M. Mühlleitner, and R. Santos, J. High Energy Phys. 09 (2022) 011.
[56] B. Grzadkowski, O. M. Ogreid, and P. Osland, J. High Energy Phys. 05 (2016) 025; 11 (2017) 002(E).
[57] K. Hagiwara, R. D. Peccei, D. Zeppenfeld, and K. Hikasa, Nucl. Phys. **B282**, 253 (1987).
[58] G. J. Gounaris, J. Layssac, and F. M. Renard, Phys. Rev. D **61**, 073013 (2000).
[59] G. J. Gounaris, J. Layssac, and F. M. Renard, Phys. Rev. D **62**, 073012 (2000).
[60] U. Baur and D. L. Rainwater, Phys. Rev. D **62**, 113011 (2000).
[61] J. F. Gunion and H. E. Haber, Nucl. Phys. **B278**, 449 (1986); **B402**, 569(E) (1993).
[62] V. Keus, S. F. King, and S. Moretti, J. High Energy Phys. 01 (2014) 052.
[63] F. Kling, S. Su, and W. Su, J. High Energy Phys. 06 (2020) 163.
[64] E. Accomando, C. Byers, D. Englert, J. Hays, and S. Moretti, Phys. Rev. D **105**, 115004 (2022).
[65] K. Desch, T. Klimkovich, T. Kuhl, and A. Raspereza, arXiv:hep-ph/0406229.
[66] J. M. No and M. Spannowsky, Eur. Phys. J. C **79**, 467 (2019).
[67] *The CLIC Potential for New Physics*, edited by J. de Blas, R. Franceschini, F. Riva, P. Roloff, U. Schnoor, M. Spannowsky, J. D. Wells, A. Wulzer, and J. Zupan, CERN Yellow Reports: Monographs Vol. 3 (CERN, Geneva, 2018), 10.23731/CYRM-2018-003.
[68] H. Al Ali, N. Arkani-Hamed, I. Banta, S. Benevedes, D. Buttazzo, T. Cai, J. Cheng, T. Cohen, N. Craig and M. Ekhterachian *et al.*, Rep. Prog. Phys. **85**, 084201 (2022).
[69] H. Burkhardt and V. I. Telnov, Report No. CERN-SL-2002-013-AP, http://cds.cern.ch/record/558830/files/sl-2002-013.pdf.
[70] J. B. Guimarães da Costa *et al.* (CEPC Study Group), arXiv:1811.10545.
[71] *The International Linear Collider Technical Design Report–Volume 2: Physics*, edited by H. Baer, T. Barklow, K. Fujii, Y. Gao, A. Hoang, S. Kanemura, J. List, H. E. Logan, A. Nomerotski, M. Perelstein *et al.*, arXiv:1306.6352.
[72] A. Abada *et al.*, Eur. Phys. J. Special Topics **228**, 261 (2019).
[73] A. Pich and P. Tuzon, Phys. Rev. D **80**, 091702(R) (2009).
[74] M. Aoki, R. Guedes, S. Kanemura, S. Moretti, R. Santos, and K. Yagyu, Phys. Rev. D **84**, 055028 (2011).
[75] P. Sanyal, Eur. Phys. J. C **79**, 913 (2019).
[76] H. Bahl, T. Stefaniak, and J. Wittbrodt, J. High Energy Phys. 06 (2021) 183.
[77] K. Cheung, A. Jueid, J. Kim, S. Lee, C. T. Lu, and J. Song, Phys. Rev. D **105**, 095044 (2022).
[78] O. Eberhardt, A. P. Martínez, and A. Pich, J. High Energy Phys. 05 (2021) 005.
[79] F. Staub, Comput. Phys. Commun. **181**, 1077 (2010).
[80] F. Staub, Comput. Phys. Commun. **185**, 1773 (2014).
[81] J. Alwall, M. Herquet, F. Maltoni, O. Mattelaer, and T. Stelzer, J. High Energy Phys. 06 (2011) 128.
[82] V. M. Budnev, I. F. Ginzburg, G. V. Meledin, and V. G. Serbo, Phys. Rep. **15**, 181 (1975).
[83] S. Frixione, M. L. Mangano, P. Nason, and G. Ridolfi, Phys. Lett. B **319**, 339 (1993).
[84] R. Ruiz, A. Costantini, F. Maltoni, and O. Mattelaer, J. High Energy Phys. 06 (2022) 114.
[85] S. Dawson, Nucl. Phys. **B249**, 42 (1985).
[86] J. F. Gunion, Y. Jiang, and S. Kraml, Phys. Rev. Lett. **110**, 051801 (2013).
[87] P. M. Ferreira, R. Santos, H. E. Haber, and J. P. Silva, Phys. Rev. D **87**, 055009 (2013).
[88] J. Heikkilä, Report No. CERN-THESIS-2015-060, 2015, https://cds.cern.ch/record/2023672/files/CERN-THESIS-2015-060.pdf.
[89] L. Bian, N. Chen, W. Su, Y. Wu, and Y. Zhang, Phys. Rev. D **97**, 115007 (2018).
[90] E. Barzi, B. Barish, W. A. Barletta, I. F. Ginzburg, and S. Di Mitri, arXiv:2203.08353, to appear in the Proceedings of the 2022 Snowmass Summer Study.
[91] I. F. Ginzburg and G. L. Kotkin, Phys. Part. Nucl. **52**, 899 (2021).
[92] G. Aad *et al.* (ATLAS Collaboration), Phys. Lett. B **816**, 136190 (2021).
[93] P. Lebiedowicz and A. Szczurek, Phys. Rev. D **91**, 095008 (2015).
[94] H. Bélusca-Maïto, A. Falkowski, D. Fontes, J. C. Romão, and J. P. Silva, J. High Energy Phys. 04 (2018) 002.
[95] M. Aaboud *et al.* (ATLAS Collaboration), Phys. Rev. D **97**, 032005 (2018).
[96] A. M. Sirunyan *et al.* (CMS Collaboration), Eur. Phys. J. C **78**, 165 (2018); **78**, 515(E) (2018).
[97] The CMS Collaboration, Report No. CMS-PAS-FTR-18-011, https://cds.cern.ch/record/2647699?ln=en.

[98] T. Ogawa, Ph.D thesis, *Graduate School of High Energy Accelerator Science, Sokendai, Japan* (2018), https://ir.soken.ac.jp/?action=repository_uri&item_id=5889&file_id=19&file_no=2.
[99] A. Cordero-Cid, J. Hernández-Sánchez, V. Keus, S. Moretti, D. Rojas, and D. Sokołowska, Eur. Phys. J. C **80**, 135 (2020).
[100] V. Keus, Phys. Rev. D **101**, 073007 (2020).
[101] A. Arhrib, R. Benbrik, J. El Falaki, M. Sampaio, and R. Santos, Phys. Rev. D **99**, 035043 (2019).
[102] P. M. Ferreira, R. Santos, and A. Barroso, Phys. Lett. B **603**, 219 (2004); **629**, 114(E) (2005).
[103] A. Barroso, P. M. Ferreira, and R. Santos, Phys. Lett. B **632**, 684 (2006).
[104] R. Boto, T. V. Fernandes, H. E. Haber, J. C. Romão, and J. P. Silva, Phys. Rev. D **101**, 055023 (2020).
[105] H. E. Haber and D. O'Neil, Phys. Rev. D **74**, 015018 (2006); **74**, 059905(E) (2006).
[106] S. Gori, H. E. Haber, and E. Santos, J. High Energy Phys. 06 (2017) 110.
[107] C. B. Braeuninger, A. Ibarra, and C. Simonetto, Phys. Lett. B **692**, 189 (2010).
[108] P. M. Ferreira, L. Lavoura, and J. P. Silva, Phys. Lett. B **688**, 341 (2010).
[109] L. J. Hall and M. B. Wise, Nucl. Phys. **B187**, 397 (1981).
[110] V. D. Barger, J. L. Hewett, and R. J. N. Phillips, Phys. Rev. D **41**, 3421 (1990).
[111] M. Aoki, S. Kanemura, K. Tsumura, and K. Yagyu, Phys. Rev. D **80**, 015017 (2009).
[112] H. E. Haber and D. O'Neil, Phys. Rev. D **83**, 055017 (2011).
[113] F. A. Berends, Phys. Lett. **16**, 178 (1965).
[114] A. Dolgov, Sov. J. Nucl. Phys. **7**, 255 (1968).
[115] C. L. Basham and P. K. Kabir, Phys. Rev. D **15**, 3388 (1977).
[116] A. D. Dolgov and L. A. Ponomarev, Sov. J. Nucl. Phys. **5**, 114 (1967).
[117] D. Fontes, M. Löschner, J. C. Romão, and J. P. Silva, Eur. Phys. J. C **81**, 541 (2021).